Protoplasma (2017) 254:997–1016
DOI 10.1007/s00709-016-1007-6

ORIGINAL ARTICLE

# β-1,3-Glucans are components of brown seaweed (Phaeophyceae) cell walls

**Sandra Cristina Raimundo**[1,2,3] · **Sivakumar Pattathil**[2] · **Stefan Eberhard**[2] · **Michael G. Hahn**[2] · **Zoë A. Popper**[1]

Received: 9 January 2016 / Accepted: 19 July 2016 / Published online: 25 August 2016


**Abstract** LAMP is a cell wall-directed monoclonal antibody (mAb) that recognizes a β-(1,3)-glucan epitope. It has primarily been used in the immunolocalization of callose in vascular plant cell wall research. It was generated against a brown seaweed storage polysaccharide, laminarin, although it has not often been applied in algal research. We conducted in vitro (glycome profiling of cell wall extracts) and in situ (immunolabeling of sections) studies on the brown seaweeds *Fucus vesiculosus* (Fucales) and *Laminaria digitata* (Laminariales). Although glycome profiling did not give a positive signal with the LAMP mAb, this antibody clearly detected the presence of the β-(1,3)-glucan in situ, showing that this epitope is a constituent of these brown algal cell walls. In *F. vesiculosus*, the β-(1,3)-glucan epitope was present throughout the cell walls in all thallus parts; in *L. digitata*, the epitope was restricted to the sieve plates of the conductive elements. The sieve plate walls also stained with aniline blue, a fluorochrome used as a probe for callose. Enzymatic digestion with an endo-β-(1,3)-glucanase removed the ability of the LAMP mAb to label the cell walls. Thus, β-(1,3)-glucans are structural polysaccharides of *F. vesiculosus* cell walls and are integral components of the sieve plates in these brown seaweeds, reminiscent of plant callose.

**Keywords** β-1,3-Glucan · Callose · Immunolabeling · LAMP mAb · Brown seaweed · Cell wall

**Abbreviations**

| | |
|---|---|
| AIR | Alcohol insoluble residue |
| CCRC | Complex Carbohydrate Research Center |
| ELISA | Enzyme-linked immunosorbent assay |
| FCSPs | Fucose-containing sulfated polysaccharides |
| Fuc | Fucose |

Handling Editor: Tsuneyoshi Kuroiwa

**Electronic supplementary material** The online version of this article (doi:10.1007/s00709-016-1007-6) contains supplementary material, which is available to authorized users.

✉ Sandra Cristina Raimundo
sraimund@skidmore.edu

Sivakumar Pattathil
siva@ccrc.uga.edu

Stefan Eberhard
seber@ccrc.uga.edu

Michael G. Hahn
hahn@ccrc.uga.edu

Zoë A. Popper
zoe.popper@nuigalway.ie

[1] Botany and Plant Science and Ryan Institute for Environmental, Marine and Energy Research, School of Natural Sciences, National University of Ireland Galway, Galway, Ireland

[2] Complex Carbohydrate Research Center, University of Georgia, Athens, GA 30602, USA

[3] Present address: Biology Department, and Skidmore Microscopy Imaging Center, Skidmore College, Saratoga Springs, NY 12866, USA

| | |
|---|---|
| Gal | Galactose |
| Glc | Glucose |
| GulA | Guluronic acid |
| KPBS | Potassium phosphate buffered saline |
| mAb | Monoclonal antibody |
| Man | Mannose |
| ManA | Mannuronic acid |
| PBST | Phosphate buffered saline tween |
| TEM | Transmission electron microscopy |
| TMB | 3,3′,5,5′-Tetramethylbenzidine |
| Xyl | Xylose |

## Introduction

Phaeophyceae, commonly known as brown seaweeds, is an almost entirely marine class of organisms belonging to the Stramenopiles (also known as Heterokonta) lineage (Patterson 1999). It includes approximately 1500 species of multicellular photosynthetic organisms (Norton et al. 1996) composed of cells surrounded by a complex carbohydrate-rich wall, features which they share with vascular plants, green (Chlorophyta) and red (Rhodophyta) algae (Popper et al. 2011; Charrier et al. 2012). Phylogenetic studies have shown that brown algae are not related to either the green or the red lineages, and therefore, their cell walls evolved independently (Yoon et al. 2004; Niklas 2004; Baldauf 2008; Michel et al. 2010a, b; Cock et al. 2010). However, the complete genome sequence of the filamentous brown alga, and model organism, *Ectocarpus siliculosus* (Cock et al. 2010), has provided unprecedented insights into the evolutionary processes that resulted not only in multicellularity and cellular differentiation but also into the uniqueness of the cell wall composition of brown algae (Coelho et al. 2012). These studies give evidence for horizontal gene transfer from other organisms, for example, of the genes responsible for the biosynthesis of some of their cell wall components (Baurain et al. 2010; Michel et al. 2010a; Stiller et al. 2009). Not surprisingly, although less complex than most vascular plants, brown algae have the highest morphological complexity of the major macroalgal groups (Charrier et al. 2012).

Brown algae can form extensive beds in the intertidal and subtidal zones of rocky shores in the northern hemisphere, playing a key role in coastal ecosystems (Lobban and Harrison 1994; Graham and Wilcox 2000; Bold and Wynne 1978). Moreover, brown algal polymers have pronounced commercial importance as sources of (1) bioactive compounds, extracted from several species (including *Fucus vesiculosus* and *Laminaria digitata*), with applications in food, pharmaceutical, and cosmetic industries; (2) phycocolloids, including alginates and sulfated polysaccharides (Stengel et al. 2011), that are important as gelling and viscosifying agents in the food and pharmaceutical industry [for example alginates have been used in the preparation of efficient gene and drug delivery systems (Zhao et al. 2012)]; and (3) biofuel applications (Wargacki et al. 2012; Enquist-Newman et al. 2014).

Brown algal cell walls are composed mainly of polysaccharides, with lower amounts of phenols, proteins, and halide compounds such as iodide (Deniaud-Bouët et al. 2014). Full characterization of algal cell walls is complicated because their composition can vary depending on factors such as species, thallus part, developmental stage, season, and habitat (Guibet et al. 2008; Kloareg and Quatrano 1988; Kropf et al. 1988; Lahaye et al. 1994; Lechat et al. 2000; Mabeau and Kloareg 1987). Nonetheless, much is already known about their composition, and the associations between their constituent polymers are becoming clearer (Deniaud-Bouët et al. 2014; Ropartz et al. 2015; Tesson and Charrier 2014). In brown algae, cellulose microfibrils account for a smaller fraction of the cell wall than in vascular plants (Naylor and Russel-Wells 1934), while alginates and sulfated fucans make up the main portion of the walls (Kloareg and Quatrano 1988). They have a higher proportion of matrix polymers in relation to the fibrillar ones, sulfated polysaccharides are abundant, and acidic sugars dominate over neutral sugars, hence the uniqueness of brown algal cell walls (Percival 1979). Alginates are linear acidic polysaccharides composed of β-1,4-D-ManA, or M blocks, and its $C_5$ epimer, α-1,4-L-GulA, or G blocks, which are present at different ratios depending on the species, seaweed part and age, and environmental conditions (Kloareg and Quatrano 1988; Percival 1979; Kim and Park 1985; Smidsrød et al. 1973). The ratios of these uronic acid residues determine the gelling characteristics of alginates; alginates with a high ratio of M blocks do not form gels in the presence of divalent cations, while G block-rich alginates form gels in the presence of calcium through the formation of the so-called egg-box junctions (Haug 1964). Fuc-containing sulfated polysaccharides (FCSPs) is the term attributed to a complex and not yet fully characterized family of sulfated polysaccharides containing α-L-fucosyl residues, usually known as fucoidan (Ale et al. 2011; Rioux et al. 2007). Algal fucoidans are very complex and heterogeneous, and their structure is species-dependent (Li et al. 2008). Their backbones are described as (1,3)-α-L-Fuc or alternating (1,3)-α-L-Fuc and (1,4)-α-L-Fuc residues (Patankar et al. 1993; Chevolot et al. 2001; Usov and Bilan 2009). Typically, FCSPs contain sulfate groups positioned on *C*-2, *C*-3, and/or *C*-4. Different monosaccharide residues such as D-Xyl, D-Gal, D-Man, and uronic acids may also be part of the FCSPs structure (Rabanal et al. 2014). While FCSPs were found to be associated with cellulose microfibrils and are thought to play an important role in brown algal wall architecture, cross-

linking other polysaccharides, this network seems to be embedded within alginates (Deniaud-Bouët et al. 2014).

In situ techniques, such as immunolocalization, are important tools in plant cell wall research, as they allow the detailed localization of specific components present in cell walls and provide important information for the study of their structure, organization, and dynamics at the cellular level (Lee et al. 2011; Domozych 2012; Willats et al. 2000). Biochemical information, routinely attained through analyses of cell wall extracts and partially or fully purified wall glycans, that allows the study of detailed composition and structure of wall polymers, is complemented by in situ techniques, as they provide additional information regarding cellular or subcellular localization of cell wall components (Knox 1997; Avci et al. 2012). Monoclonal antibodies (mAbs) are monospecific probes that bind to epitopes present in cell wall polymers, and are also useful as screening tools for high-throughput characterization of specific cell wall and biomass extracts (Pattathil et al. 2012; Moller et al. 2007, 2008, 2012). Almost all mAbs currently available for plant cell wall research were generated against epitopes present in vascular plant cell walls, but some have been shown to bind to epitopes present in the walls of freshwater (Domozych et al. 2011; Domozych and Lambiasse 2009; Domozych et al. 2007; Estevez et al. 2008) and marine green algae (Estevez et al. 2009; Fernández et al. 2010). Although mAbs have been specifically generated against epitopes present in brown (Vreeland 1970, 1972; Jones et al. 1988) and red seaweed (Vreeland et al. 1992) cell wall polysaccharides, and localization studies were performed using these mAbs (Vreeland et al. 1984; Green et al. 1993), they are no longer available to the scientific community. New mAbs have been generated against brown seaweed fucoidans, and different localization patterns associated with different epitope specificities were reported (Torode et al. 2015). Using an alternative approach, mAbs generated against plant cell wall polysaccharides were shown to bind to epitopes present in brown seaweed cell walls, and have thallus-specific localization patterns (Raimundo et al. 2016). Thus, continuing research on seaweeds is producing new knowledge that will lead to a better understanding of wall architecture as well as the cellular properties of polysaccharides in commercially valuable (marine) algae.

LAMinarin Pentaose, or LAMP (LAMP2H12H7, Biosupplies 400-2), is one of the 200+ commercially available mAbs that recognize epitopes present in vascular plant cell wall glycans (Pattathil et al. 2010, 2015), and are extensively used by the scientific community both for glycome profiling (Pattathil et al. 2012; Moller et al. 2007, 2012) and immunolocalization studies (Avci et al. 2012). Most frequently applied to plant cell wall studies, the LAMP mAb resin-embedded was found to bind to different thallus parts of *F. vesiculosus* sections (Raimundo et al. 2016). Although this mAb was generated against laminarin extracted from *L. digitata*, and its epitope is characterized (Meikle et al. 1991, 1994), immunolabeling studies where the LAMP mAb is used are almost nonexistent for algae.

*F. vesiculosus* (Fucales) and *L. digitata* (Laminariales) are brown seaweeds common in the intertidal zone of rocky coastlines in the temperate northern hemisphere (Bold and Wynne 1978). *F. vesiculosus*, commonly known as bladder wrack, is a midlittoral species. It has a dichotomously branched thallus (Fig. 1a) with a discoid holdfast, a narrow stipe (Fig. 1b), a flattened blade with a central midrib (Fig. 1c) and, often, air bladders (Fig. 1d). Specialized reproductive organs of this dioecious species, called receptacles, are located at the periphery of the algal thallus (Fig. 1e) (Lee 2008; Graham and Wilcox 2000; Lobban and Harrison 1994). Laminariales, commonly known as kelps, include the largest known seaweeds, such as *Macrocystis* that can grow up to 50 m long. Within this order, *L. digitata* is a key species that forms extensive beds from the upper sublittoral fringe downwards (Lobban and Harrison 1994). *L. digitata* is ecologically important as it provides a habitat for many smaller macroalgae (e.g., for *Mastocarpus stellatus* and *Palmaria palmata*) (Schaal et al. 2016) as well as providing habitat and food for many marine animals like fish, crustaceans, mollusks, and polychaetes (Schultze et al. 1990). *L. digitata* also accumulates iodine from seawater in higher amounts than other seaweeds (Nitschke and Stengel 2015) and plays an important role in iodine emissions, as well as a mediator of coastal iodine fluctuations (Nitschke et al. 2013). *L. digitata* has a diploid sporophytic thallus (Fig. 1f) differentiated into a holdfast which anchors the alga to a hard substratum, a smooth and flexible stipe (Fig. 1g), and a long, large blade, with an intercalary meristem located at the junction of the stipe and blade (Fig. 1h) (Graham and Wilcox 2000; Lobban and Harrison 1994). Unlike *F. vesiculosus*, which forms reproductive receptacles at the tips of the fronds, the reproductive organs of *L. digitata* are clustered in patches, or sori, usually scattered over the blade (Fig. 1i). Sporangia are formed inside the sori, producing haploid spores that after release into the seawater, will settle and develop into dioecious gametophytes (Schiel and Foster 2006).

In this study, we used the LAMP mAb to perform in situ immunolocalizations in different thallus parts of *F. vesiculosus* and *L. digitata*. We highlight the importance of this rarely used mAb as a valuable molecular marker for the study of cell walls of brown seaweeds. The immunolabeling results, combined with the absence of labeling when sections were pretreated with an endo-β-(1,3)-glucanase prior to immunolabeling, confirm the presence of the β-(1,3)-glucan epitope recognized by the LAMP mAb as a component of *F. vesiculosus* cell walls. This epitope was shown to be present in all thallus parts of this species. The observed labeling pattern for *L. digitata* differed, inasmuch as labeling was restricted to the sieve plates of the conductive elements in this species. Although callose has been assumed to be the main component of sieve plates in brown

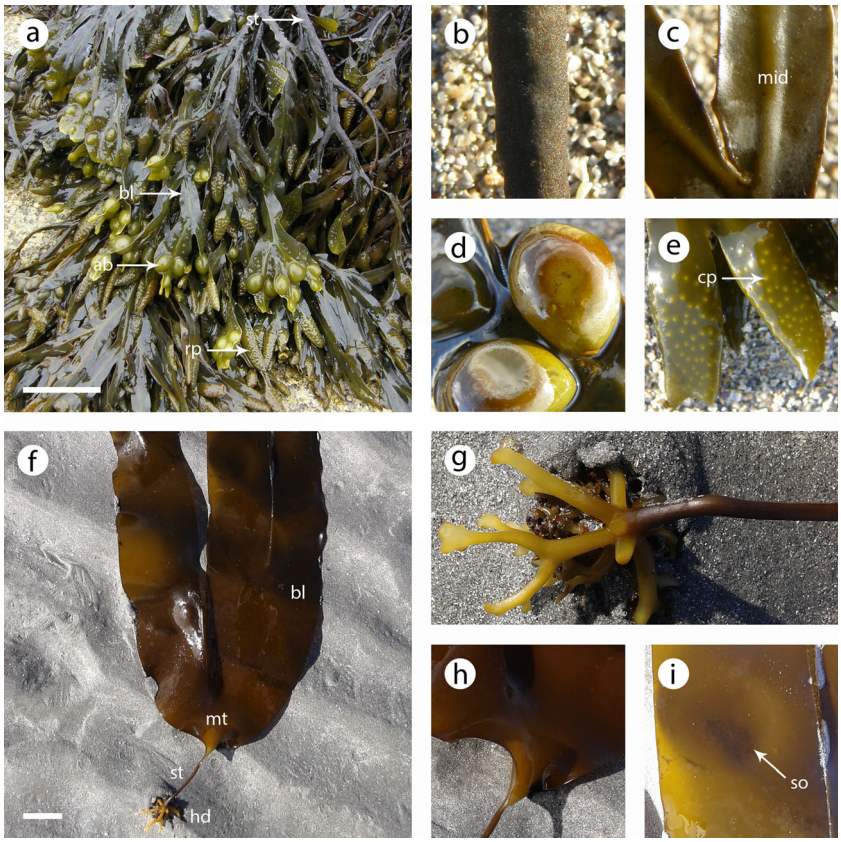


**Fig. 1** Morphology of the brown seaweeds *Fucus vesiculosus* and *Laminaria digitata*. **a** General appearance of *F. vesiculosus*. The thallus is differentiated into holdfast (not shown), stipe (**b**), and blade (**c**) with midrib and air bladders (**d**). The reproductive structures, receptacles (**e**), inside of which the conceptacles are formed, are found at the thallus tips. **f** General appearance of *L. digitata*. The sporophytic thallus is differentiated into holdfast, stipe (**g**), and blade, with an intercalary meristem located at the junction of the stipe and blade (**h**). Sori appear as dark patches scattered over the blade (**i**). *ab* air bladder, *bl* blade, *cp* conceptacle; *hd* holdfast, *mid* midrib, *mt* meristem, *rp* receptacle, *so* sori, *st* stipe. *Scale bars* = 5 cm

seaweeds since they were first observed (Smith 1939; Yamanouchi 1908), sieve plate composition had not been fully detailed in the seaweeds. Although we cannot affirm that the wall component labeled by the LAMP mAb is indeed callose, our results demonstrate the presence of β-(1,3)-glucan epitopes as part of the walls of the brown seaweeds studied here. These epitopes either reflect the presence of callose in the cell walls or are part of another polysaccharide that has the same epitope as part of its structure.

## Materials and methods

### Algal material

Male and female specimens of the brown macroalga *Fucus vesiculosus* Linnaeus and sporophytes of *Laminaria digitata* (Hudson) J. V. Lamouroux (Phaeophyceae, Heterokontophyta) were collected at Finavarra, Co. Clare (53° 09′ 25″ N, 09° 06′ 58″ W), on the west coast of Ireland in July 2014, washed with tap water, and cleaned of visible epiphytes and/or grazers.

### Monoclonal antibodies

Monoclonal antibodies generated against different cell wall glycans were obtained as hybridoma cell culture supernatants from stocks at the Complex Carbohydrate Research Center (CCRC). The CCRC, PN, JIM, and MAC series are available from CarboSource (www.carbosource.net). LAMP2H12H7 and BG-1 antibodies are available from Biosupplies (Parkville, Victoria, Australia, www.biosupplies.com.au). A list of the antibodies used, including links to the online database, Wall*Mab*DB (www.wallmabdb.net), is provided in Supplementary Table T1.

### Preparation of algal material for light microscopy

Algal material was fixed and embedded as previously described (Coimbra et al. 2007) with minor modifications. Small pieces of different parts of the seaweed thallus (2–5 mm) were cut and put in a fixative solution [2 % (*v*/*v*) paraformaldehyde; 0.25 % (*v*/*v*) glutaraldehyde; 0.025 M PIPES buffer; 0.001 % (*v*/*v*) Tween 80; pH 7.2]. The material was fixed for 2 h at room temperature followed by an overnight incubation at 4 °C. Samples were washed with 0.025 M PIPES buffer, pH 7.2, for 10 min, followed by a second wash for 20 min. Dehydration was done in a graded ethanol series [25 % (*v*/*v*), 35 % (*v*/*v*), 50 % (*v*/*v*), 70 % (*v*/*v*), 80 % (*v*/*v*), 90 % (*v*/*v*), and 3 times with 100 %] with 15 min for each grade, and infiltration was performed by a sequential immersion in different proportions of 100 % ethanol and LR White Resin (medium grade, Agar Scientific, Cambridge, UK) over

6 days (ethanol/LR White proportion per day was 3:1; 2:1; 1:1; 1:2; 1:3; 0:1). After the final resin change, samples were placed either in gelatin capsules or polyethylene molds (Electron Microscopy Sciences, Hatfield, PA, USA) depending on the preferred sample orientation, and fresh LR White was added. The capsules were hermetically sealed while the molds were covered with Aclar embedding film (Electron Microscopy Sciences, Hatfield, PA, USA), and all the samples were placed in an oven at 60 °C for 2 days.

### Preparation of algal material for electron microscopy

Freshly collected algal material was cut into small pieces (2–4 mm) and placed in a fixative solution of 1 % (*v*/*v*) glutaraldehyde in filtered seawater for 60 min. After washing 3 times with filtered seawater for 5 min for each wash, samples were incubated for 2 h in a postfixative solution of 1 % (*v*/*v*) osmium tetroxide in filtered seawater. Samples were kept on ice throughout the procedures. After a second washing step performed as described above, the samples were brought to room temperature. Dehydration, embedding, and polymerization steps were performed in the same way as for light microscopy.

### Light microscopy—immunohistochemistry

Immunolabeling was executed as previously reported (Avci et al. 2012). In brief, semithin sections (250 nm) were cut with a Leica EM UC6 ultramicrotome (Leica Mikrosysteme GmbH, Vienna, Austria), at room temperature, with a histodiamond knife (DiATOME, Hatfield, PA, USA). Sections were mounted on glass slides (Fisherbrand Superfrost Plus, Fisher Scientific, Pittsburgh, PA, USA) and dried at 50 °C for 1 min. The sections used for future reference regarding anatomical information were stained with toluidine blue; a drop of 1 % (*w*/*v*) toluidine blue in 1 % (*w*/*v*) sodium borate was put on the sections for 20 s (McCully et al. 1980), washed with distilled water, and dried. The sections used for immunolabeling were blocked with 3 % (*w*/*v*) nonfat dry milk (instant nonfat dry milk, Publix) in potassium phosphate buffered saline (KPBS) (0.01 M potassium phosphate, pH 7.1, containing 0.5 M NaCl) for 30 min, and then incubated for 60 min with LAMP2H12H7 mAb (Biosupplies, Parkville, Victoria, Australia) (concentration used according to the manufacturer's instructions). Negative controls were incubated with KPBS instead of the mAb. The sections were washed with KPBS, 3 × 5 min, and incubated with goat anti-mouse IgG conjugated with AlexaFluor 488 (Invitrogen Molecular Probes, Eugene, OR, USA) secondary antibody (1:100 in KPBS) for 90 min, after which the sections were washed with KPBS, 2 × 5 min. After a final wash with distilled water (5 min), the sections were mounted with Citifluor antifade mounting medium AF1 (Electron Microscopy Sciences, Hatfield, PA, USA) and covered with a coverslip.

### Transmission electron microscopy—immunogold labeling

Sample preparation for transmission electron microscopy (TEM) was performed as described previously (Domozych et al. 2007) with some modifications. Thin sections (70 nm) of osmicated algal material were collected on formvar-coated (EMS, Hatfield, PA, USA) copper grids (for regular TEM observation) and on nickel grids. Sections on nickel grids were treated for 2 min with 5 % (*v*/*v*) hydrogen peroxide, washed with deionized water, treated for 10 min with 0.26 % (*w*/*v*) ammonium chloride, and rewashed. Sections were blocked with 1 % (*w*/*v*) blotting grade blocker (Bio-Rad) in phosphate buffered saline with 5 % (*v*/*v*) Tween 20 (PBST) for 30 min at room temperature. After washing with deionized water, the sections were incubated at 33 °C for 2 h with a 1:200 dilution (in PBST) of the LAMP mAb. After a wash with deionized water, sections were reblocked for 30 min, washed, and incubated for 90 min at 33 °C with a 1:50 dilution (in PBST) of EM goat anti-mouse IgG secondary antibody conjugated with 10 nm gold particles (Ted Pella, Inc., Redding, CA, USA). After washing with deionized water, both copper and nickel sections were stained with conventional uranyl acetate/lead citrate: grids were incubated with 1 % (*w*/*v*) uranyl acetate for 5 min, washed with deionized water, incubated with 1 % (*w*/*v*) lead citrate for 2–3 min, and washed with deionized water previously boiled for 4 min (and cooled overnight).

### Enzymatic digestion

Sections on slides were incubated at 40 °C with 5 U of endo-1,3-β-D-glucanase (purified from *Trichoderma* sp., Megazyme, Bray, Ireland) in 50 mM acetate buffer (pH 4.5) for 60 min, washed with KPBS, and then labeled with the LAMP mAb, as described above.

### Aniline blue staining

Aniline blue fluorochrome (Biosupplies, Parkville, Victoria, Australia) was prepared according to the manufacturer's instructions. The stock solution of 0.1 mg $mL^{-1}$ of the fluorochrome in distilled water was diluted in KPBS (1:3), and semithin sections (250 nm) of the resin-embedded algal tissue were incubated for 30 min at 20 °C. After washing with distilled water, the sections were mounted with Citifluor antifade mounting medium AF1 (Electron Microscopy Sciences, Hatfield, PA, USA) and covered with a coverslip.

### Microscopy

Immunolabeling was observed with a Nikon Eclipse 80i (Nikon Instruments, Melville, NY, USA) microscope equipped with epifluorescence optics. Images were captured

with a Nikon DS-Ri1 camera (Nikon Instruments, Melville, NY, USA) using NIS-Elements Basic Research software and assembled with Adobe Photoshop Elements 11.0 (Adobe Systems, San Jose, CA, USA) software. The aniline blue and the postenzyme-digested immunolabeling imaging were performed with a Nikon Eclipse E400 (Nikon Instruments, Melville, NY, USA) microscope equipped with epifluorescence optics, and the images were captured with an Olympus DP72 camera using CellSens software (Olympus Inc., Melville, NY, USA). TEM micrographs were taken with a Zeiss-Libra 120 transmission electron microscope (Carl Zeiss SMT Inc., Thornwood, NY, USA). Images were captured with a Cantega G2 camera (Olympus Soft Imaging Solutions GmbH, Münster, Germany), using iTEM 5.1 TEM Imaging Platform.

### Cell wall extraction

Algal cell walls were extracted based on previously described protocols for extracting vascular plant cell walls (Pattathil et al. 2012). The algal material was ground to a fine powder in liquid nitrogen and the powder was suspended in 80 % (*v*/*v*) ethanol, shaken overnight at room temperature, and centrifuged at 3000×*g* for 15 min. The supernatant was discarded and the pellet washed with 80 % (*v*/*v*) ethanol followed by final washing steps using 100 % ethanol and acetone. The final alcohol insoluble residue (AIR) was air-dried in a hood for 24 h and subjected to sequential extractions with increasingly harsh reagents as described below. All extractions were carried out in suspensions at 10 mg $mL^{-1}$ based on the starting weight of the AIR used, with constant mechanical stirring (200 rpm) at 70 °C for 24 h. After each extraction, the supernatant was collected by centrifugation at 3000×*g* for 10 min and stored at 4 °C. The AIR was extracted sequentially with 50 mM ammonium oxalate (pH 5), 50 mM sodium carbonate ($Na_2CO_3$) containing 0.5 % (*w*/*v*) sodium borohydride ($NaBH_4$) (pH 10), 1 M potassium hydroxide (KOH) containing 1 % (*w*/*v*) $NaBH_4$, 4 M KOH containing 1 % (*w*/*v*) $NaBH_4$, and 100 mM sodium chlorite, and the pelleted residue was treated once more with 4 M KOH containing 1 % (*w*/*v*) $NaBH_4$ (KOHPC). The 1-M KOH, 4-M KOH, and 4-M KOHPC fractions were neutralized using glacial acetic acid. All extracts were dialyzed (Spectra/Por 3 Dialysis Membrane 3500 Da MWCO, Spectrum Laboratories Inc., Rancho Dominguez, CA, USA) against three changes of deionized water at 4 °C for a total of 48 h, freeze-dried, and weighed. The extracts were stored at room temperature in a desiccator containing a drying agent (silica) prior to further analysis.

### Total sugar estimation

Total sugar content of the cell wall extracts were estimated using the phenol-sulfuric acid method in microplates (Masuko et al. 2005; Dubois et al. 1956). Briefly, the cell wall extracts were dissolved in deionized water at a gravimetric concentration of 0.2 mg $mL^{-1}$; 100 μL of 5 % (*v*/*v*) phenol was added to 100 μL of each dissolved extract, followed by 500 μL 18 M sulfuric acid ($H_2SO_4$), and the samples incubated at room temperature for 20 min in a fume hood. Samples were transferred to 96-well plates (Costar 3598, Corning Inc., NY, USA). Optical densities was read at $A_{490\ nm}$ with a Model 680 Microplate Reader (Bio-Rad Laboratories, Inc., Hercules, CA, USA), using the Microplate Manager Version 5.2 Build 103 software. A standard curve prepared using D-glucose (Glc) solutions at different concentrations (5 to 50 μg) was used to calculate the Glc equivalents present in the extracts.

### Enzyme-linked immunosorbent assay

Enzyme-linked immunosorbent assays (ELISAs) were carried out as described previously (Pattathil et al. 2010). Briefly, 96-well plates (Costar 3598, Corning Inc., NY, USA) were loaded with 50 μL of aliquots of diluted seaweed extracts (10 μg/mL in distilled water). Tamarind xyloglucan (Megazyme, Bray, Ireland) probed with the CCRC-M104 mAb was used as a positive control, while distilled water was added to the negative control wells. After being left to dry overnight at 37 °C, the plates were incubated with 200 μL of 1 % (*w*/*v*) nonfat dry milk (instant nonfat dry milk, Publix Super Market, USA) in Tris-buffered saline (2 mM Tris-base, 8 mM Tris-HCl, pH 7.6 containing 100 mM sodium chloride) for 1 h. The aspiration and washing steps employed an ELx405 VRS Microplate Washer (BioTek Instruments Inc., Winooski, VT, USA); incubations were done at room temperature. After aspirating the blocking solution, 50 μL of undiluted hybridoma supernatant of the mAbs were added (LAMP and BG-1 were diluted 1:70 in 0.1 M Tris-buffered saline) to the wells and incubated for 1 h. After aspiration of the antibody solutions and a 3 times wash step with 200 μL of 0.1 % (*w*/*v*) nonfat dry milk in Tris-buffered saline, the wells were incubated for 1 h with 50 μL of horseradish peroxidase-conjugated goat anti-mouse IgG or goat anti-rat IgG secondary antibodies (Sigma-Aldrich, St. Louis, MO, USA), diluted 1:5000 in wash buffer. Antibody solutions were aspirated and the wells were washed 5 times with 200 μL of wash buffer. TMB peroxidase substrate Kit (SK-4400, Vector Laboratories, Inc., Burlingame, CA, USA) was prepared based on the manufacturer's instructions, and 50 μL was added to each well and incubated for 30 min. Fifty microliters of 1 N of $H_2SO_4$ was added to stop the reaction and the optical density was immediately read as the difference between $A_{450}$ and $A_{655}$ using a Model 680 Microplate Reader (Bio-Rad Laboratories, Inc., Hercules, CA, USA), controlled

by the Microplate Manager Version 5.2 Build 103 software. The reading for the corresponding negative control well was subtracted from each sample well. ELISA results were presented as a heat map using R-Console software (Team RDC 2011).

## Results

### Immunolabeling

This study focused on examining the cells and tissues of different thallus parts of two brown seaweeds, *F. vesiculosus* and *L. digitata*, for the presence of 1,3-β-glucans using the LAMP mAb, which had been generated against laminarin (Meikle et al. 1991). Immunolocalization showed strong and specific labeling patterns in every tissue examined for both species (Figs. 2, 3, 4, 5, 6, 7, and 8), with the exception of the meristoderm cells. The following sections detail the immunolocalization patterns observed in each seaweed.

#### *Fucus vesiculosus*

The stipe sections of *F. vesiculosus* showed a generalized positive labeling with the LAMP mAb throughout the medullary cell walls. The longitudinal sections show the elongated primary filament cells (Fig. 2b, f) that appear round in cross section (Fig. 2a, d). Nonspecific labeling or autofluorescence was not detected in any of the thallus parts (Figs. 2c; 3c, d; and 4c, d). The LAMP mAb labeled all of the cell walls of the primary filament cells, as can be readily observed in the immunostained cross section (Fig. 2e). In longitudinal sections, the presence of cross-walls at the end of each contiguous medullary primary filament becomes visible; these are sieve elements or sieve tubes (Fig. 2f), and the LAMP mAb bound particularly strongly to these walls (Fig. 2g). Labeling was also observed in the blade and air bladder tissues (Fig. 3a, b). The blade tissues showed a generalized labeling in the cortex cell walls but not in the meristoderm (Fig. 3e, f). The medullary cell walls were also labeled, particularly the thick cell walls of the secondary hyphae (Fig. 3g, h). The dense medullary filament cell walls in the midrib region of the blade were also labeled with the LAMP mAb (Fig. 3i, j), as were the cell walls of the air bladder (Fig. 3k, l). Both male (Fig. 4a) and female (Fig. 4b) receptacle tissues showed a general labeling throughout the cortex (Fig. 4e, f) and medulla cell walls (Fig. 4g, h). However, as observed in other tissues, the meristoderm cell walls did not label (Fig. 4f). Generalized labeling was also observed for the conceptacles, where both male and female paraphyses cell walls were labeled (Fig. 4j, l). However, while in the male antheridia only the inner cell walls labeled and the outer walls did not (Fig. 4i, j), the three walls that surround each female oogonium, i.e., the exochite, mesochite, and endochite, were labeled (Fig. 4k, l).

#### *Laminaria digitata*

Labeling by the LAMP mAb was observed in the holdfast cell walls of *L. digitata* (Fig. 5a), namely in the medullary cells (Fig. 5c), although the labeling was not contiguous (Fig. 5d). The stipe cells appear round in cross section (Fig. 6a, d) and no labeling was observed, with the exception of the thick cross-walls (Fig. 6e), typically found in the sieve plates. Longitudinal sections allowed distinction between the hyphae and the trumpet hyphae, also known as sieve cells (Fig. 6b, f). The LAMP mAb specifically labeled the thick cell walls in the sieve plates of the trumpet hyphae, which are the conducting elements in *L. digitata* (Fig. 6g). The blade and the stipe have a similar anatomy (Figs. 6b and 7a), although the hyphae are more disperse in the blade, with more extracellular mucilage between the cells, and they are not organized so distinctively parallel in the blade as they are in the stipe (Fig. 7a, e). Similarly to the stipe, positive labeling with the LAMP mAb was detected in the thick walls of the sieve plates, and some labeling was also present inside the hyphal cells (Fig. 7f). In contrast, a different labeling pattern was observed on the fertile blade (Fig. 7b, g): the sorus cortex cell walls labeled intensely, but no labeling was observed in the sporangia (Fig. 7h). Nonspecific labeling or autofluorescence was also not detected in any of the thallus parts (Figs. 5b, 6c, and 7c, d).

Immunogold labeling confirmed the presence of the epitope recognized by the LAMP mAb in the sieve plates of the trumpet hyphae (Fig. 8). The sieve plates observed with TEM appear as dense punctate structures (Fig. 8a, c); the gold particles showed a parallel distribution in both external sides of the plate (Fig. 8b, d), although with an uneven distribution, as more particles accumulated in certain areas of the sieve plate (Fig. 8e).

### Aniline blue staining

Aniline blue has been used to stain β-glucans in other studies (Falter et al. 2015; Herburger and Holzinger 2015; Tsirigoti et al. 2015; Park et al. 2015; Wood and Fulcher 1984). So we also used the fluorochrome to stain *F. vesiculosus* and *L. digitata*. In the case of *F. vesiculosus*, no staining with aniline blue was observed in the algal tissues (Supplementary Fig. S1). On the other hand, aniline blue staining was observed for *L. digitata*, being localized exclusively to some of the cross-walls of the medullary trumpet hyphae (Fig. 9a, b). Some autofluorescence at the wavelength used to observe aniline blue was visible in the negative control (Fig. 9c), but appeared to be localized to the interior of the cortex cells and therefore did not interfere with the observations. In the trumpet hyphae of the medullary tissue (Fig. 9d, f), aniline blue staining was found to be specifically localized to the sieve plates (Fig. 9e, g).

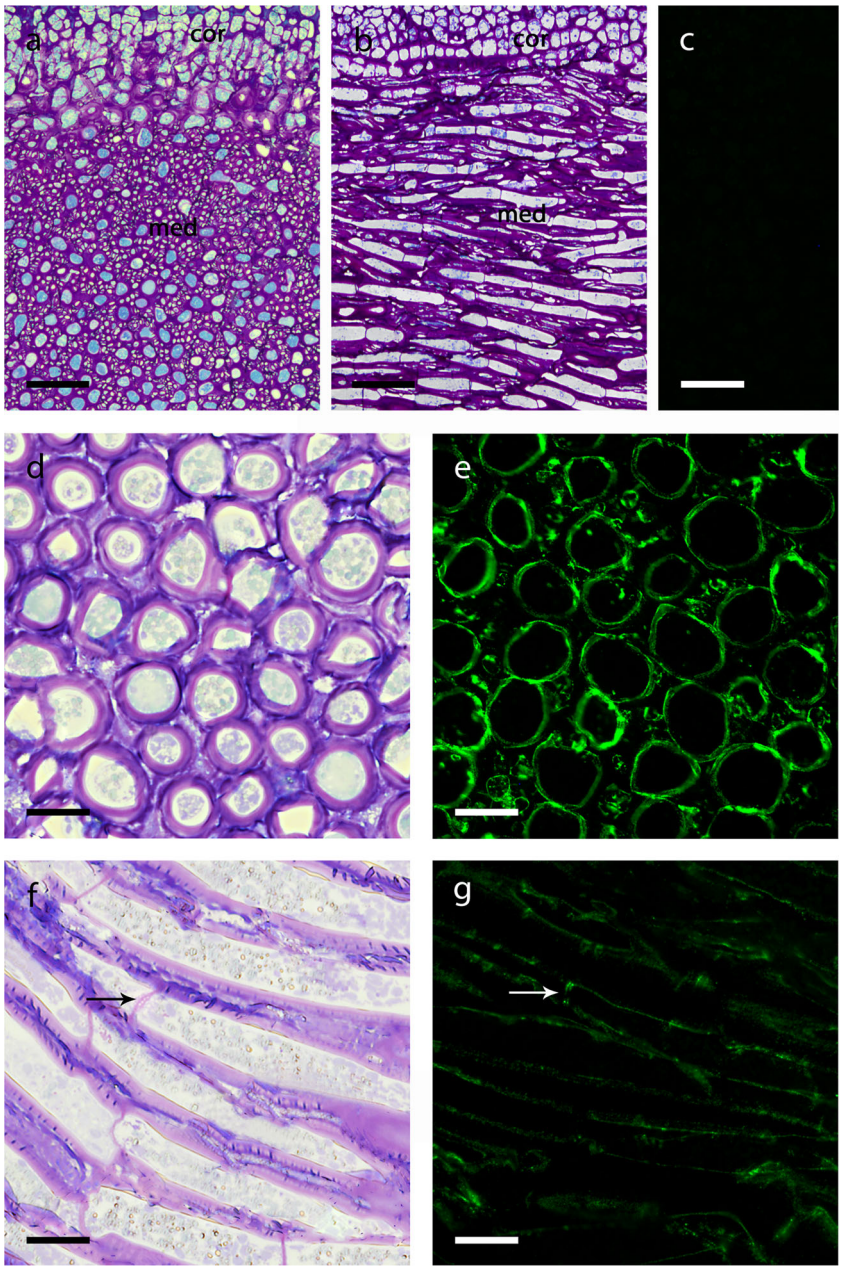


**Fig. 2** Sections of *F. vesiculosus* stipe immunolabeled with the LAMP mAb and stained with toluidine blue. **a** Morphology of a stipe cross section stained with toluidine blue. **b** Morphology of a stipe longitudinal section stained with toluidine blue. **c** Negative control where no primary mAb was used during the immunolabeling. **d** Cross section of medulla cells stained with toluidine blue. **e** LAMP mAb labeling showed binding to the medulla cell walls. **f** Medulla cells in longitudinal section stained with toluidine blue. The *arrow* points to a sieve plate. **g** LAMP mAb labeling showed binding to the medulla cell walls. The *arrow* points to the labeling of a sieve plate. *cor* cortex, *med* medulla. *Scale bars*: **a**, **b** = 100 μm, **c**–**g** = 25 μm

## Enzymatic digestion

Pretreatment of sections with endo-1,3-β-D-glucanase resulted in the enzymatic digestion of the epitope recognized by the LAMP mAb in both species (Fig. 10). Labeling was observed in the positive controls, where no enzyme was used, localized to the cell walls in *F. vesiculosus* (Fig. 10b) and to the sieve plates in *L. digitata* (Fig. 10e). Labeling with the LAMP mAb was abolished when the sections were pretreated with the enzyme prior to immunostaining, and only autofluorescence inside the cells was observed (Fig. 10c, f), a labeling pattern that was similar to the negative controls (Fig. 10a, d).

## Glycome profiling

The cell walls of *F. vesiculosus* and *L. digitata* were subjected to glycome profiling (Pattathil et al. 2012) in order to obtain an overall picture of the presence of glycan structures in these two brown seaweeds that are similar to those present in vascular plants. Glycome profiling uses a large and diverse collection of mAbs directed against noncellulosic glycan epitopes typically found in vascular plants (Pattathil et al. 2010). The results demonstrated that *F. vesiculosus* walls contain diverse glycan epitopes in common with arabinogalactans of vascular plants, similar to a previous report (Raimundo et al. 2016), while *L. digitata* walls contain very few epitopes

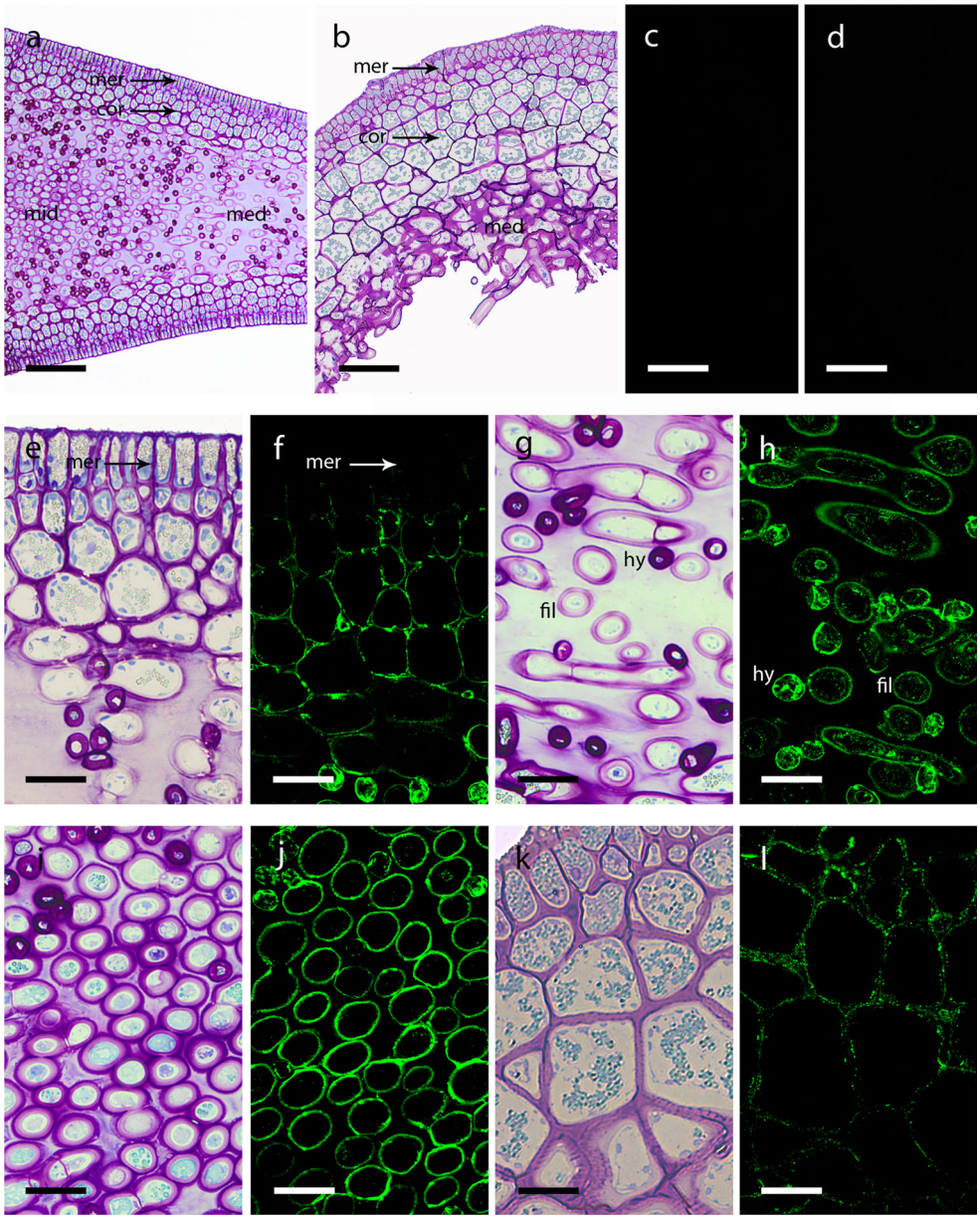


**Fig. 3** Cross sections of *F. vesiculosus* blade and air bladder immunolabeled with the LAMP mAb and stained with toluidine blue. **a** Morphology of a blade section stained with toluidine blue. **b** Morphology of the air bladder stained with toluidine blue. **c**, **d** Negative controls of the blade (**c**) and of the air bladder (**d**) where no primary mAb was used during the immunolabeling. **e** Cortex region stained with toluidine blue. **f** LAMP mAb labeling showed binding to the cortex cell walls but not to the meristoderm. **g** Medulla region stained with toluidine blue. **h** LAMP mAb labeling showed binding to the medullary hyphae and filament cell walls. **i** Medulla region of the midrib stained with toluidine blue. **j** LAMP mAb labeling showed binding to the midrib cell walls. **k** Air bladder stained with toluidine blue. **l** LAMP mAb labeling showed binding to the air bladder cell walls. *cor* cortex, *fil* primary filament, *hy* secondary hypha, *med* medulla, *mer* meristoderm, *mid* midrib. *Scale bars*: **a**, **b** = 100 μm, **c**–**l** = 25 μm

of this type (Fig. 11). The walls of both brown seaweeds examined in this study also contained glycan structures recognized by some xylan-directed mAbs (Fig. 11). No signal was detected in the profiles for the LAMP mAb.

## Discussion

In this study, we describe for the first time the presence and distribution of a (1,3)-β-glucan epitope in the cell walls of the brown seaweeds *F. vesiculosus* and *L. digitata* using immunolocalization with LAMP, a mAb specific to this epitope (Meikle et al. 1991, 1994). This antibody proved to be an excellent marker for the cell walls in most of the thallus parts studied, showing it to be a valuable tool for in situ studies of brown seaweeds. Staining with the aniline blue fluorochrome correlated with LAMP mAb labeling of the sieve plates, confirming that β-(1,3)-glucan deposits, reminiscent of plant callose, are integral components of the sieve plates. However, the fluorochrome did not stain the majority of the cell walls which labeled with the LAMP mAb. This suggests that a cell wall polymer that bears the β-(1,3)-glucan epitope as part of its structure was recognized with the LAMP antibody but that it was not able to be stained with aniline blue, possibly due to limitations of the fluorochrome in comparison to the mAb. Pretreatment of tissue sections with an endo-1,3-β-D-glucanase prior to immunostaining resulted in the loss of binding by the LAMP mAb, thereby confirming the presence of

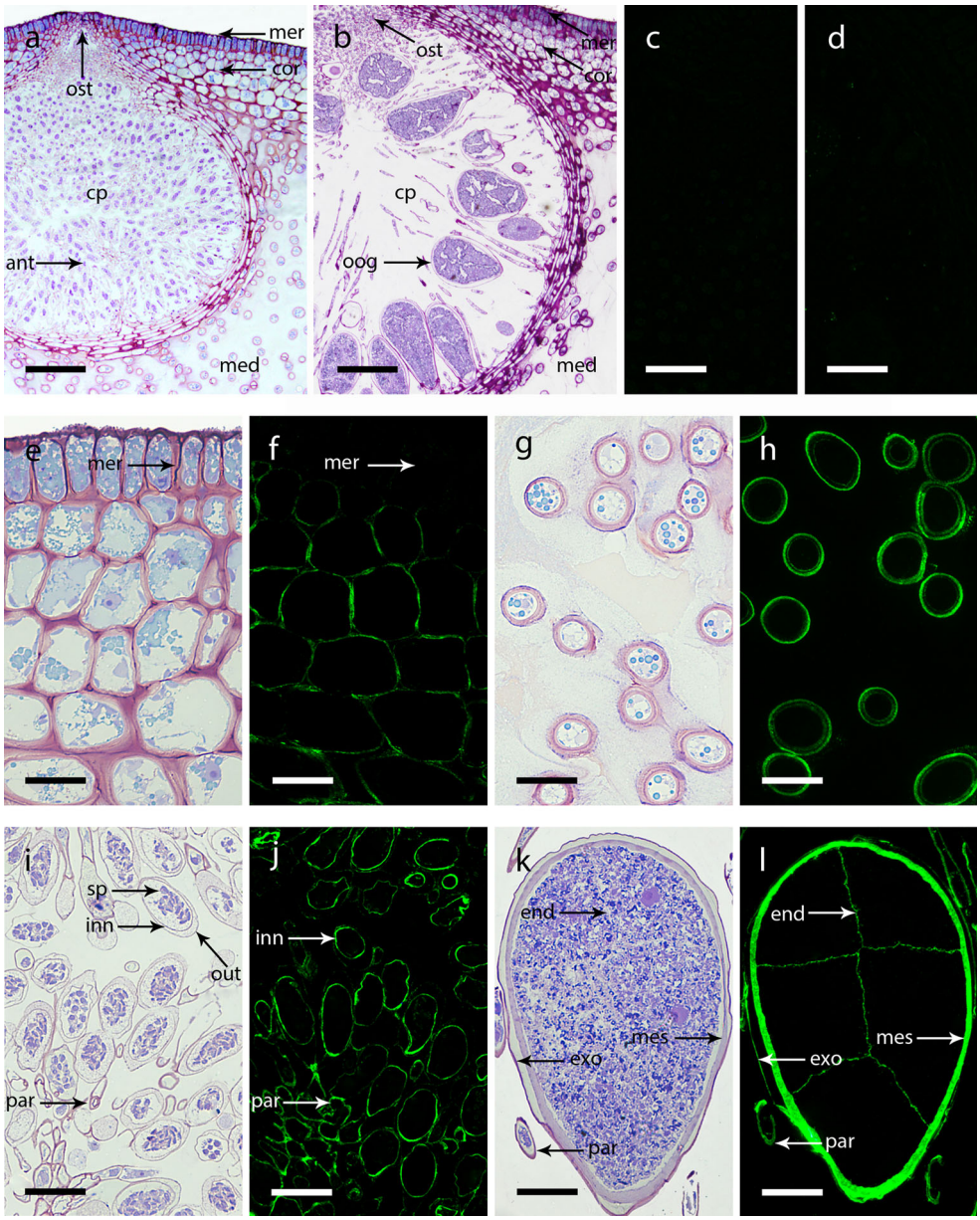


**Fig. 4** Cross sections of *F. vesiculosus* receptacles immunolabeled with the LAMP mAb and stained with toluidine blue. **a** Male receptacle stained with toluidine blue. **b** Female receptacle stained with toluidine blue. **c**, **d** Negative controls of the male (**c**) and female conceptacles (**d**) where no primary mAb was used during the immunolabeling. **e** Cortex region stained with toluidine blue. **f** LAMP mAb labeling showed binding to the cortex cell walls but not to the meristoderm. **g** Medulla region stained with toluidine blue. **h** LAMP mAb labeling showed binding to the medulla cell walls. **i** Part of the male conceptacle stained with toluidine blue. **j** LAMP mAb labeling showed binding to the male paraphyses and antheridia inner cell walls. **k** Oogonium from a female conceptacle stained with toluidine blue. **l** LAMP mAb labeling showed binding to the female paraphyses and oogonia exochite, mesochite, and endochite cell walls. *ant* antheridium, *cor* cortex, *cp* conceptacle, *end* endochite, *exo* exochite, *inn* inner wall, *med* medulla, *mer* meristoderm, *mes* mesochite, *oog* oogonium, *ost* ostiole, *out* outer wall, *par* paraphyse, *sp* sperm cells. *Scale bars*: **a**, **b** = 100 μm, **c**–**l** = 25 μm

(1,3)-β-glucan epitope in the seaweed cell walls. Interestingly, the glycome profiles did not show LAMP mAb binding to any cell wall extracts from either of these brown algae (Fig. 11). This apparent dichotomy could be explained by the inability of any of the reagents used for the preparation of the wall extracts to solubilize the 1,3-β-glucans from the wall samples. It has been noted previously that a considerable percentage of the callose present in certain plants and tissues cannot be solubilized readily in alkali, but only with concentrated (sulfuric or formic) acids (Kauss 1989). Similarly, high yields of laminarin were achieved only after using hydrochloric acid (Kadam et al. 2015). Therefore, it is possible that the extraction methods performed for the glycome profiling did not extract the epitopes recognized by the LAMP mAb. Alternatively, the β-glucan epitope recognized by the antibody could reside on a polymer that is too small to adhere to the plastic surface of the ELISA plates (Pattathil et al. 2012).

### LAMP mAb epitope distribution—storage polysaccharides

Phototrophic eukaryotes use different molecular forms of glucans as storage polysaccharides and their intracellular localization varies depending on the lineage of the organism (Suzuki and Suzuki 2013). Laminarin is a glucan that consists of β-1,3-linked chains with occasional β-1,6-linked branches (Beattie et al. 1961; Read et al. 1996). It is considered to be the main storage glucan in brown seaweeds, located in the

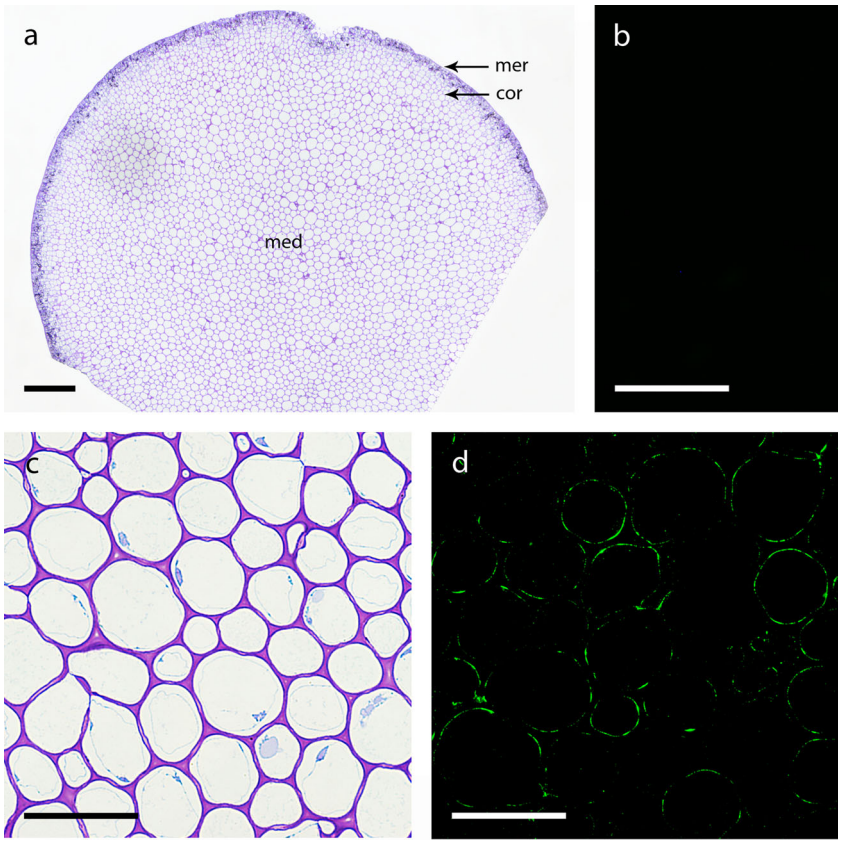


**Fig. 5** Cross sections of *L. digitata* holdfast immunolabeled with the LAMP mAb and stained with toluidine blue. **a** Morphology of a cross section stained with toluidine blue. **b** Negative control where no primary mAb was used during the immunolabeling. **c** Medulla cells stained with toluidine blue. **d** LAMP mAb labeling showed binding to the medulla cell walls. *cor* cortex, *med* medulla, *mer* meristoderm. *Scale bars*: **a** = 100 μm, **b**–**d** = 50 μm

cytoplasm, and was not thought to be a cell wall component (Mian and Percival 1973; Quatrano and Stevens 1976). Experiments with radioactive carbon showed that laminarin, as well as mannitol, are storage sugars in the brown alga *Eisenia bicyclis* and may be interchangeable compounds, analogous to sucrose and starch in plants (Yamaguchi et al. 1966). The use of the LAMP antibody outside vascular plants and associated callose labeling is very scarce. There are reports on the use of this mAb in brown seaweeds, namely the application of immunogold labeling to study the ultrastructure and development of the pyrenoids in the chloroplasts of four species (Tanaka et al. 2007); however, the authors did not present evidence for labeling of the cell walls of the species studied. The LAMP antibody has also been used to study storage glucans in chlorarachniophytes (McFadden et al. 1997), a group of small wall-less amoeboid eukaryotes (Hibberd and Norris 1984; Ludwig and Gibbs 1989) that have enclosed a green algal endosymbiont, retaining it as a photosynthetic organelle (McFadden et al. 1994, 1997). Immunolabeling showed that the storage polysaccharides produced by the endosymbiont, (1,3)-β-glucans, are stored within the vacuole of the host cell (McFadden et al. 1997) and nowhere else. In comparison with the existing reports, our results show only weak labeling inside the cells, which was specifically observed inside the medullary primary filaments in *F. vesiculosus* blade (Fig. 3h) and inside the medullary hyphae in *L. digitata* blade (Fig. 7f). Although some labeling inside the cells could be expected, because the LAMP mAb can recognize nonbranched parts of laminarin, no labeling was observed in the cells of any of the other thallus parts. Our results suggest that, although the LAMP mAb was generated toward laminarin, the (1,3)-β-glucan epitope it recognizes is predominantly part of a cell wall polymer, rather than a storage polymer.

### LAMP mAb epitope distribution—link to callose

The LAMP2H12H7 mAb was reported as an anti-(1,3)-β-glucan antibody, or simply LAMP. It was generated against commercially available laminarin that originated from *L. digitata*. The LAMP mAb recognizes a (1,3)-β-glucan epitope composed of five consecutive Glc residues (βGlc-(1,3)-βGlc-(1,3)-βGlc-(1,3)-βGlc-(1,3)-Glc); it has no cross-reactivity with β-(1,4)-glucan (cellulose) or to (1,3)(1,4)-β-D-glucan (mixed linkage glucan) (Meikle et al. 1991, 1994), and as far as we are aware, no other cross-reactivities of this mAb have been reported. This epitope is typically found in callose, a polymer characterized by a linear (1,3)-β-glucan chain with some (1,6)-branches (Aspinall and Kessler 1957). Callose is present in specific cells and subcellular locations in vascular plants including phloem elements, cell plates, plasmodesmata, root hairs, and tracheids; its

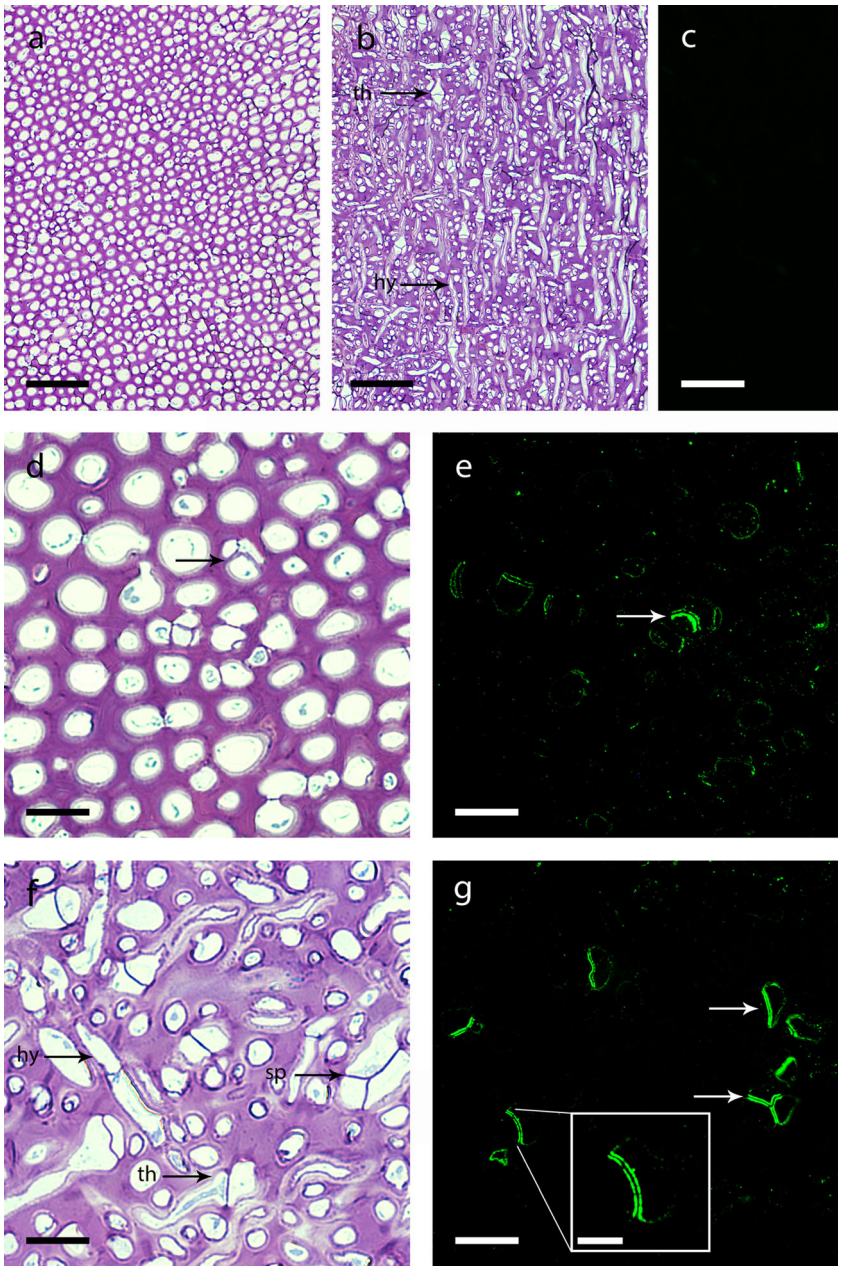


**Fig. 6** Sections of *L. digitata* stipe immunolabeled with the LAMP mAb and stained with toluidine blue. **a** Cross section of the medulla region stained with toluidine blue. **b** Longitudinal section of the medulla region stained with toluidine blue. **c** Negative control where no primary mAb was used during the immunolabeling. **d** Medulla cells in cross section, stained with toluidine blue. Some sieve plates are visible (*arrows*). **e** LAMP mAb labeling showed binding to the sieve plates (*arrow*). **f** Medulla cells in a longitudinal section stained with toluidine blue. The *arrows* indicate the hyphae and the trumpet hyphae sieve plates. **g** LAMP mAb labeling showed specific binding to the trumpet hyphae sieve plates (*arrows*). A close up of a sieve plate is shown in the box. *hy* hypha, *sp* sieve plate, *th* trumpet hypha. *Scale bars*: **a**, **b** = 100 μm, **c**–**g** = 25 μm

biosynthesis can also be induced by wounding, pathogen infection, and stress (Stone and Clarke 1992; Kauss 1996). In experimental terms, callose is histochemically identified by its ability to bind to aniline blue dye or fluorochrome, to be recognized by the (1,3)-β-glucan-specific mAb, and by its susceptibility to degradation by (1,3)-β-glucan-specific enzymes (Stone 2009).

The LAMP mAb has primarily been used as a callose-specific antibody in vascular plants, for immunolocalization studies related to pollen tubes (Geitmann et al. 1995; Mollet et al. 2013; Ferguson et al. 1998), plasmodesmata (Radford et al. 1998), pathogen-infected cells (Chowdhury et al. 2014), and tracheid cell walls (Altaner et al. 2010). Similarities exist between the distribution of callose for vascular plants and seaweeds. For example, callose was recently reported to be part of the defense mechanisms of filamentous brown seaweeds with (1,3)-β-glucans deposited postinfection in pathogen-host contact areas (Tsirigoti et al. 2015), and β-(1,3)-glucans have been found in *Fucus* embryo cell walls (Novotny and Forman 1975). Furthermore, similarly to vascular plants, Laminariales also have a system for the translocation of photoassimilates (Schmitz and Lobban 1976); they have sieve elements that consist of cells with perforated terminal end walls, or sieve plates, arranged in long continuous longitudinal rows to form sieve tubes throughout the thallus, except in the holdfast (Van Went et al. 1973; Sykes 1908). The ends of each sieve plate can be expanded so it resembles a

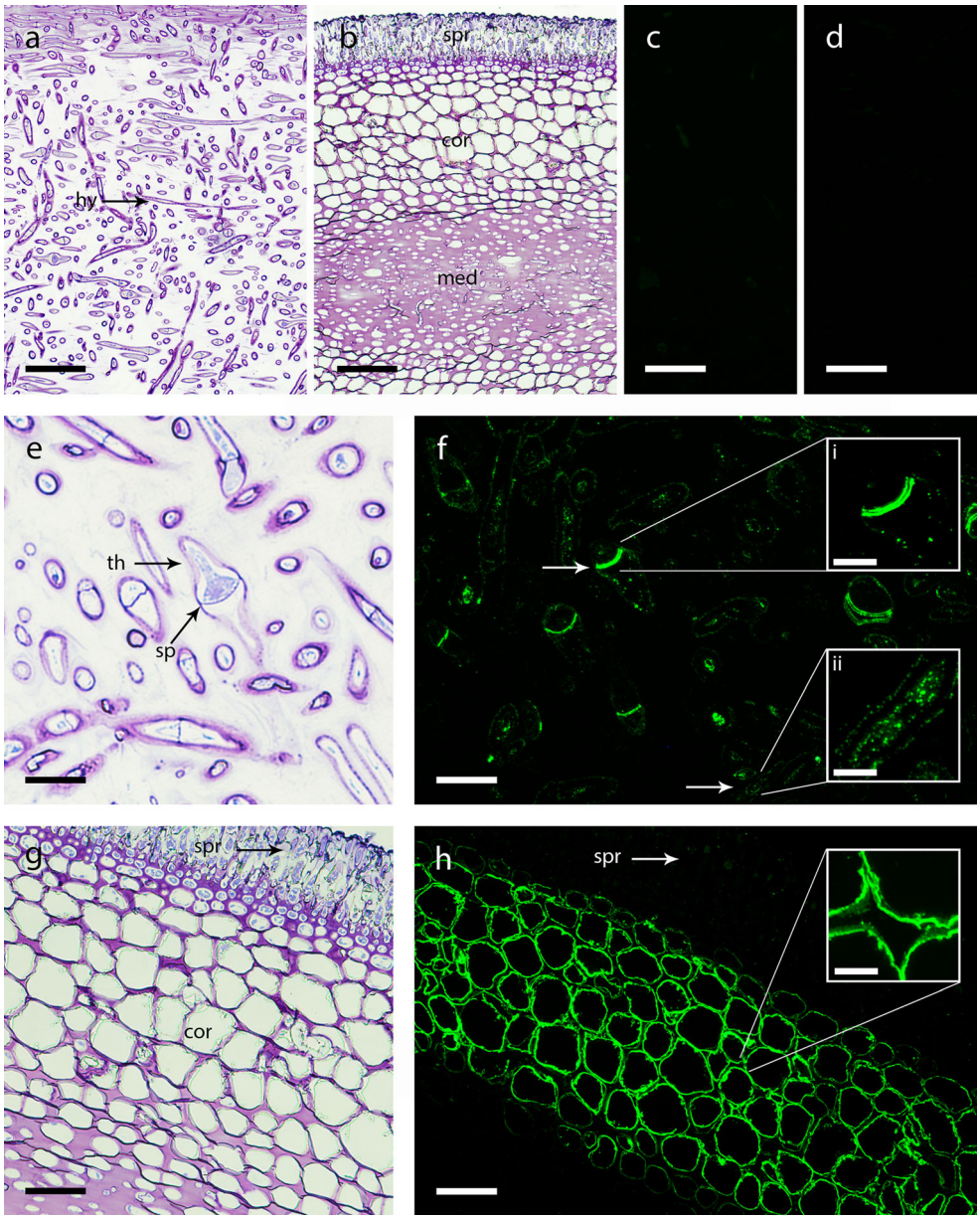


**Fig. 7** Cross sections of *L. digitata* blade and fertile blade immunolabeled with the LAMP mAb and stained with toluidine blue. **a** Morphology of the medulla region stained with toluidine blue. **b** Morphology of the fertile blade stained with toluidine blue. **c**, **d** Negative controls of the blade (**c**) and of the sorus (**d**) where no primary mAb was used during the immunolabeling. **e** Medulla cells of the blade stained with toluidine blue, the *arrows* point to the sieve plates of the trumpet hyphae. **f** LAMP mAb labeling showed binding to the sieve plates and inside the cells (*arrows*). A close up of the labeling *i* of a sieve plate and *ii* inside the hyphae cells. **g** Sorus stained with toluidine blue. **h** LAMP mAb labeling showed binding to the sorus cortex cell walls but not to the sporangia. A detail of the labeling is shown. *cor* cortex, *hy* hyphae, *med* medulla, *sp* sieve plate, *spr* sporangia, *th* trumpet hyphae. *Scale bars*: **a**, **b** = 100 μm, **c**–**h** = 25 μm

trumpet, hence the name trumpet hyphae. Although some researchers considered the trumpet filaments as artifacts (Van Went and Tammes 1973), they are well described (Graham and Wilcox 2000; Lee 2008) and we observed these structures clearly (Figs. 6b, f and 7a, e). The sieve plates have a role in controlling vesicle trafficking along the sieve tubes driven by turgor pressure, recently reported to be controlled by a regulatory mechanism of buffering that happens through wall swelling (Knoblauch et al. 2016). Likewise, Fucales have sieve elements in the central medullary filaments with smaller pores, although they do not form trumpet-shaped hyphae (Moss 1983). They are smaller and not so easily detected, but were visible in the toluidine blue-stained longitudinal sections (Fig. 2b, f). There are several reports of the presence of callose in the sieve elements in brown seaweeds (Yamanouchi 1908; Smith 1939; Van Went et al. 1973; Schmitz and Srivastava 1976; Lee 2008), although that presence was not unambiguously proven. Our results show that a polysaccharide that resembles plant callose is present in the sieve plates of both *F. vesiculosus* (Fig. 2g) and *L. digitata* (Figs. 6e, g; 7f; and 8b, d) based on positive labeling with the LAMP mAb, commonly used to localize callose in vascular plants. Nonetheless, we cannot precisely affirm that the polymer recognized is callose. The β-(1,3)-glucan epitope could also be part of a different polysaccharide that has not yet been described.

To compare and complement our observations for the distribution of a (1,3)-β-glucan in seaweed cell walls, we also stained sections with the aniline blue fluorochrome, frequently used for the detection of callose (Evans et al. 1984; Stone et al.

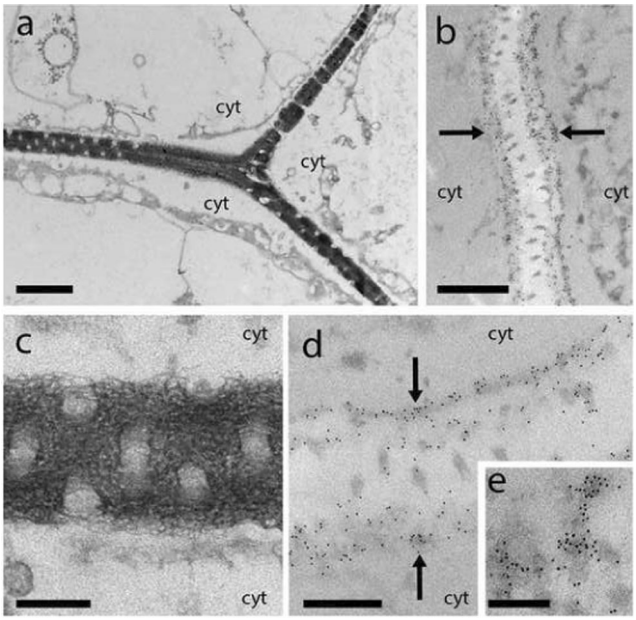


**Fig. 8** Transmission electron micrographs of the trumpet hyphae sieve plates of *L. digitata* blade longitudinal sections (**a**–**e**) immunogold labeled with the LAMP mAb (**b**, **d**, **e**). **a** Sieve plates have a characteristic punctate dense structure. **b** Gold particles are visible along the sieve plates (*arrows*). **c** Close up of the sieve plate and the same area labeled (**d**), showing the gold particles distributed along the two external sides of the sieve plate (*arrows*). **e** The gold particles accumulate more densely in some areas. *Scale bars*: **a**, **b** = 1000 nm, **c**, **d** = 200 nm, **e** = 100 nm

1984). Aniline blue did not stain any of the cell walls of *F. vesiculosus* (Supplementary Fig. S1) with the exception of the sieve plates (Fig. 9). The results were surprising because the LAMP mAb showed broad labeling of the cell walls of *F. vesiculosus* (Figs. 2, 3, and 4). This apparent discrepancy could be due to differing sensitivities of the two methods for (1,3)-β-glucan detection. One of the biggest advantages of the use of mAbs is that they bind to their epitopes with high affinity and thus are able to detect and localize specific glycan epitopes even when they are present at low amounts within the cell walls (Raimundo et al. 2016). On the other hand, a fluorochrome such as aniline blue requires a threshold level of the compound to be present before it can be stained and thereby recognized. This could be why aniline blue stained the sieve plates, which contain higher levels of callose, but not the cell walls. Other possibilities include the fact that aniline blue binding may be influenced by the interaction of the glycan with the surrounding wall components; for instance, quenching of aniline blue fluorescence by the presence of phenolic compounds was reported (Smith and McCully 1978). Phenolic compounds are known to be present at particularly high levels (~2.5 % of total dry weight) in brown seaweeds (Audibert et al. 2010), and are present in the cell walls (Deniaud-Bouët et al. 2014; Schoenwaelder 2008) where they may inhibit aniline blue from binding to and staining the cell walls.

After the complete sequencing of the brown alga *E. siliculosus* genome (Cock et al. 2010), bioinformatic and phylogenetic approaches allowed the identification of three homologous genes from a family that contains eukaryotic (1,3)-β-glucan synthases that have significant similarities (35 % sequence identity) to plant callose synthases (Michel et al. 2010b). This finding suggests that brown

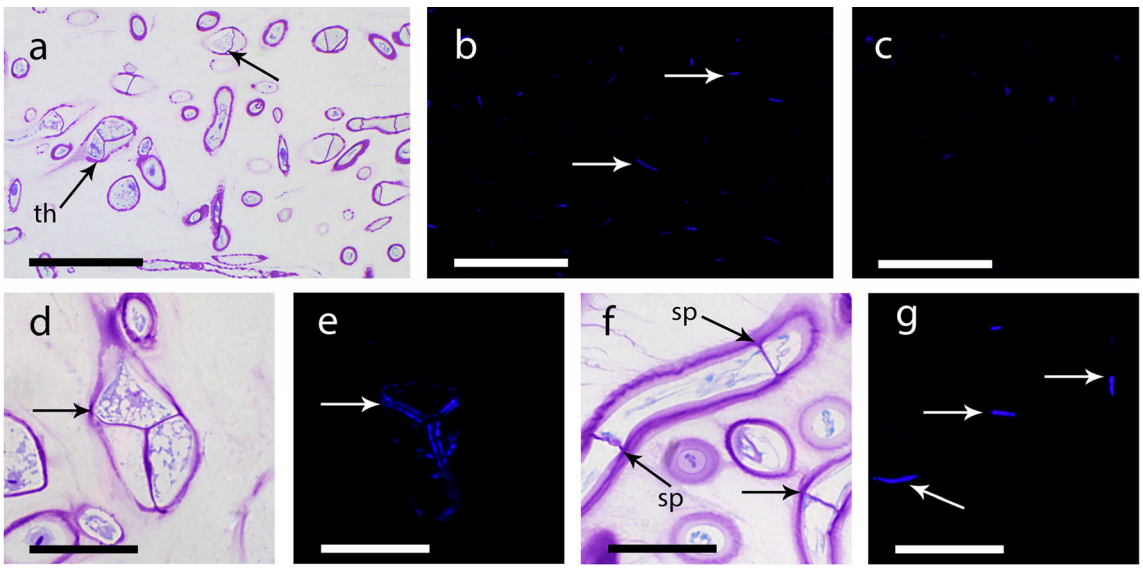


**Fig. 9** Longitudinal sections of *L. digitata* blade stained with toluidine blue (**a**, **d**, **f**) and aniline blue (**b**, **e**, **g**). **a** Morphology of the medulla region stained with toluidine blue. **b** Aniline blue staining of the medulla. **c** Negative control, no aniline blue was used. **d** Detail of the intersection of trumpet hyphae stained with toluidine blue. **e** Detail of the aniline blue staining of the sieve plates in the trumpet hyphae. **f** Detail of the longitudinal appearance of trumpet hyphae stained with toluidine blue. **g** Detail of the aniline blue staining of the sieve plates. *sp* sieve plate, *th* trumpet hyphae. *Scale bars*: **a**–**c** = 50 μm, **d**–**g** = 20 μm

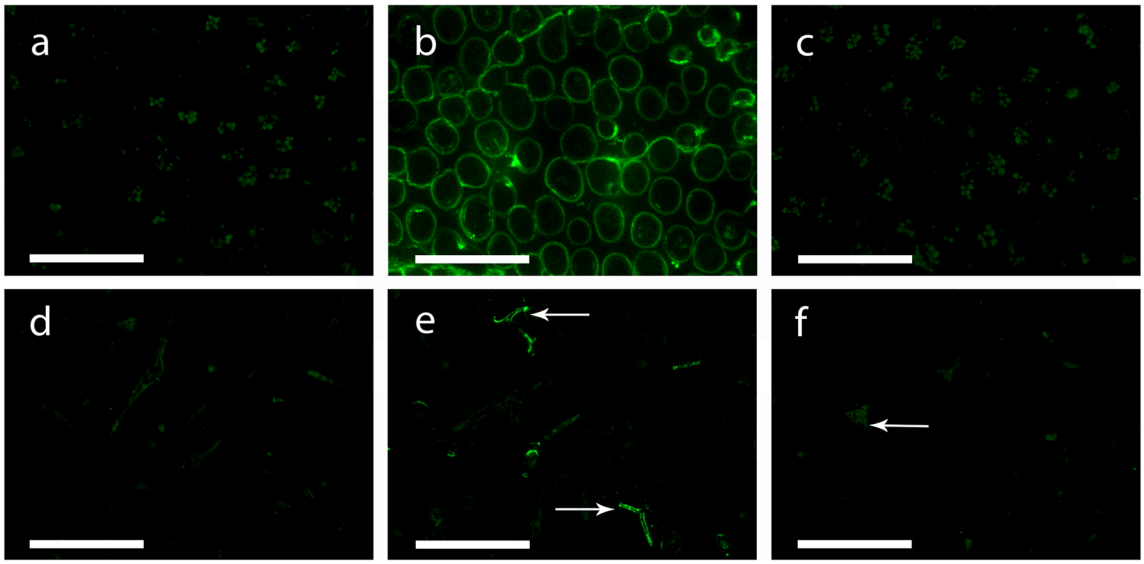


**Fig. 10** Sections of *F. vesiculosus* (**a**–**c**) and *L. digitata* (**d**–**f**) blades immunolabeled with the LAMP mAb (**b**, **c**, **e**, **f**) and after digestion with endo-1,3-β-D-glucanase (**c**, **f**). **a** *F. vesiculosus* negative control where no primary mAb was used. **b** *F. vesiculosus* positive control, where immunolabeling was performed without enzyme treatment; the labeling of the medullary cell walls is visible. **c** No labeling was observed in *F. vesiculosus* when sections were preincubated with the enzyme. **d** *L. digitata* negative control where no primary mAb was used. **e** *L. digitata* positive control, where immunolabeling was performed without enzyme treatment; the labeling of the sieve plates of the trumpet hyphae is visible (*arrows*). **f** No labeling was observed in *L. digitata* when sections were preincubated with the enzyme. The *arrow* points to an area where a sieve plate is located. *Scale bars* = 50 μm

seaweeds have the genetic machinery necessary to synthesize callose. Our results support the possibility that callose may be present both in sieve plates of the conductive elements, as well as in other brown algal cell walls, although we cannot exclude the possibility that the epitope recognized by the LAMP mAb in the seaweeds may be part of another polysaccharide, especially since the brown seaweeds are evolutionarily distantly related to vascular plants, and have different cell wall compositions.

### LAMP mAb epitope distribution—cell walls

Our results show the distribution of the (1,3)-β-glucan epitope in brown seaweeds, including the species that was used to generate the LAMP mAb. A broad distribution of the epitope was observed throughout the cell walls of the two species studied here. Interestingly, it was often observed that some areas of the cell walls remained unlabeled such that labeling was not uniform (Figs. 2e, g; 3f, l; 4f; and 5d). These gaps with no labeling might indicate the presence of cell wall microdomains. Nonuniform staining with aniline blue has been attributed to differences in the architectural organization of the wall polymers (Smith and McCully 1978), so this could be the case for the LAMP mAb as well, specially in the areas that were not labeled, which seem to coincide with the location of plasmodesmata. Moreover, it was rarely observed, but some cross-walls did not label (Fig. 2g). This could be indicative of the phenomenon of callose turnover, which has been described for vascular plants. The molecular weight limit for the molecules that can go through plasmodesmata is determined by the degradation and synthesis of callose at the neck region of plasmodesmata upon external or internal signals, resulting in the reversible decrease of the diameter of the plasmosdesmata (Zavaliev et al. 2011).

Immunogold labeling performed on *L. digitata* blade sections confirmed the immunofluorescence observations, in that gold particles were found in the sieve plates (Fig. 8b, d), although their distribution was uneven (Fig. 8e). Callose has an essential role in sieve plate development in vascular plants, being deposited beneath the plasma membrane on both sides of the sieve plate wall, forming a collar that encloses each plasmodesmata (Xie et al. 2011). The differences in the gold particle distribution observed could correlate to the presence of cell wall microdomains that contain callose, as has been shown to be present around vascular plant plasmodesmata (Knox and Benitez-Alfonso 2014).

Immunolocalization of *F. vesiculosus* showed a broad labeling of all of the cortex and medulla cell walls, regardless of the thallus part. In this species, two types of filaments are present: the primary filaments, with a larger diameter, and the thicker secondary hyphae (McCully 1965), that labeled more strongly, and are especially visible in the blade (Fig. 3f, h). These hyphae are formed through a process of secondary thickening (Pennington 1937), where cortical and medullary cells give rise to long, thick-walled hyphae, more slender than the medullary filaments, with very narrow protoplasm, which grow into the mucilage of the

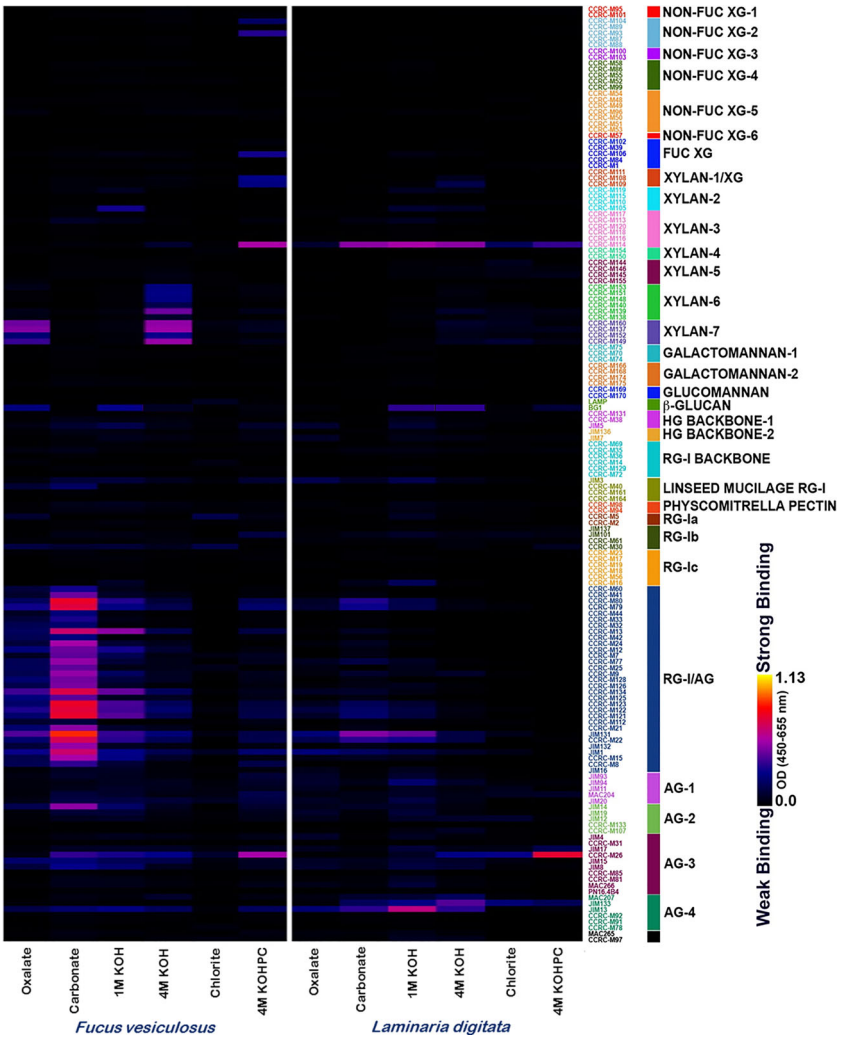


**Fig. 11** Glycome profiling using cell wall extracts from whole thallus of *F. vesiculosus* and *L. digitata*. The data is presented as a heat map, resulting from the ELISA screening using 155 plant cell wall glycan-directed monoclonal antibodies. The detailed list of the antibodies used is shown on the *right panel*, color-coded as groups based on a hierarchical clustering of the cell wall glycans recognized by each antibody group (Supplementary Table T1). The ELISA signal strength is displayed by a *black-blue-red-yellow* scale, with *black* indicating the absence of binding and *yellow* showing strongest binding. Labels at the bottom indicate the reagents used for each extraction step for each species

medulla. The hyphae also stained more intensely with toluidine blue than the filaments (Fig. 3e, g). Their thick walls were intensely labeled with the LAMP mAb suggesting that the (1,3)-β-glucan epitope is a major component of these walls. The fact that the epitope was present in all walls including in the male and female conceptacle cell walls, except the outer walls of the antheridia, suggests that this epitope is part of a structural cell wall polymer. However, in *L. digitata*, no cell walls labeled, with the exception of the trumpet hyphae sieve plates and the cortex that supports the sporangia within the fertile blade. It is difficult to interpret the physiological meaning of the observed epitope distribution patterns. However, it is tantalizing to speculate that they may be related to changes in cell function associated with the life cycle. On the other hand, both *F. vesiculosus* and *L. digitata* are marine species from the same class Phaeophyceae that evolved into the orders Fucales and Laminariales, respectively, adapted to different habitats, and have to withstand different environmental stresses. The labeled polymer may play a role in contributing to desiccation tolerance of *F. vesiculosus*, the intertidal species, in a similar way to recently reported for callose in the freshwater green alga *Klebsormidium flaccidum* (Herburger and Holzinger 2015).

The LAMP mAb is highly selective and specific for (1,3)-β-glucans and, as such, is rarely utilized in cell wall localization studies within vascular plants or other organisms, except when callose is a specific target of the research, or when the walls are known to contain such glucans [e.g., yeast cell walls (Humbel et al. 2001)]. Our studies broaden the possibilities for the application of this mAb and show that the LAMP mAb is a valuable tool for the detection and localization of β-glucans in the cell walls of brown seaweeds. Based on our labeling results, the β-glucan that the LAMP mAb recognizes is part of the cell walls of brown seaweeds, rather than a storage polysaccharide, and the observed distribution patterns of this epitope are unique and widespread. This suggests that these β-glucans are part of a structural component of the walls of these brown seaweeds.

**Acknowledgments** The authors thankfully acknowledge the technical support provided by Professor David Domozych (Skidmore Microscopy Imaging Center, Skidmore College) with the TEM and by Dr. Kerry Thompson (Center for Microscopy and Imaging, NUI Galway) with the aniline blue imaging. The authors thank Prof. Azeddine Driouich (Center for Plant Glycobiology, Université de Rouen, France) and Dr. Maria Tuohy (Biochemistry, NUI Galway) for helpful comments during the preparation of this manuscript. The financial support was provided by the Science Foundation Ireland (SFI) (Research Frontiers Programme, grant 11/RFP/EOB/3345 awarded to Z.A.P). The generation of the CCRC series of mAbs was supported by the US National Science Foundation Plant Genome Program (Awards DBI-0421683 and IOB-0923992 to M.G.H.).

**Compliance with ethical standards**

**Conflict of interest** The authors declare that they have no conflict of interest.

## References

Ale MT, Mikkelsen JD, Meyer AS (2011) Important determinants for fucoidan bioactivity: a critical review of structure-function relations and extraction methods for fucose-containing sulfated polysaccharides from brown seaweeds. Mar Drugs 9(10):2106–2130. doi:10.3390/md9102106

Altaner CM, Tokareva EN, Jarvis MC, Harris PJ (2010) Distribution of (1→4)-β-galactans, arabinogalactan proteins, xylans and (1→3)-β-glucans in tracheid cell walls of softwoods. Tree Physiol 30(6):782–793. doi:10.1093/treephys/tpq021

Aspinall GO, Kessler G (1957) The structure of callose from the grape vine. J Soc Chem Ind Lond 1957:1296

Audibert L, Fauchon M, Blanc N, Hauchard D, Gall EA (2010) Phenolic compounds in the brown seaweed *Ascophyllum nodosum*: distribution and radical-scavenging activities. Phytochem Anal 21:399–405. doi:10.1002/pca.1210

Avci U, Pattathil S, Hahn MG (2012) Immunological approaches to plant cell wall biomass characterization: immunolocalization of glycan epitopes. In: Himmel ME (ed) Biomass conversion: methods and protocols, vol 908. Methods in molecular biology. Humana, pp 73–82. doi:10.1007/978-1-61779-956-3_7

Baldauf SL (2008) An overview of the phylogeny and diversity of eukaryotes. J Syst Evol 46(3):263–273. doi:10.3724/SP.J.1002.2008.08060

Baurain D, Brinkmann H, Petersen J, Rodríguez-Ezpeleta N, Stechmann A, Demoulin V, Roger AJ, Burger G, Lang BF, Philippe H (2010) Phylogenetic evidence for separate acquisition of plastids in Cryptophytes, Haptophytes, and Stramenopiles. Mol Biol Evol 27(7):1698–1709. doi:10.1093/molbev/msq059

Beattie A, Hirst EL, Percival E (1961) Studies on the metabolism of the Chrysophyceae. Comparative structural investigations on leucosin (chrysolaminarin) separated from diatoms and laminarin from the brown algae. Biochem J 79:531–537

Bold HC, Wynne MJ (1978) Introduction to the algae: structure and reproduction. Prentice-Hall biological sciences. Prentice-Hall, New Jersey

Charrier B, Le Bail A, Reviers B (2012) Plant Proteus: brown algal morphological plasticity and underlying developmental mechanisms. Trends Plant Sci 17(8):468–477. doi:10.1016/j.tplants.2012.03.003

Chevolot L, Mulloy B, Ratiskol J, Foucault A, Colliec-Jouault S (2001) A disaccharide repeat unit is the major structure in fucoidans from two species of brown algae. Carbohydr Res 330(4):529–535. doi:10.1016/S0008-6215(00)00314-1

Chowdhury J, Henderson M, Schweizer P, Burton RA, Fincher GB, Little A (2014) Differential accumulation of callose, arabinoxylan and cellulose in nonpenetrated versus penetrated papillae on leaves of barley infected with *Blumeria graminis* f. sp. *hordei*. New Phytol 204:650–660. doi:10.1111/nph.12974

Cock JM, Sterck L, Rouzé P, Scornet D, Allen AE, Amoutzias G, Anthouard V, Artiguenave F, Aury J-M, Badger JH, Beszteri B, Billiau K, Bonnet E, Bothwell JH, Bowler C, Boyen C, Brownlee C, Carrano CJ, Charrier B, Cho GY, Coelho SM, Collén J, Corre E, Silva C, Delage L, Delaroque N, Dittami SM, Doulbeau S, Elias M, Farnham G, Gachon CMM, Gschloessl B, Heesch S, Jabbari K, Jubin C, Kawai H, Kimura K, Kloareg B, Küpper FC, Lang D, Le Bail A, Leblanc C, Lerouge P, Lohr M, Lopez PJ, Martens C, Maumus F, Michel G, Miranda-Saavedra D, Morales J, Moreau H, Motomura T, Nagasato C, Napoli CA, Nelson DR, Nyvall-Collén P, Peters AF, Pommier C, Potin P, Poulain J, Quesneville H, Read B, Rensing SA, Ritter A, Rousvoal S, Samanta M, Samson G, Schroeder DC, Ségurens B, Strittmatter M, Tonon T, Tregear JW, Valentin K, Von Dassow P, Yamagishi T, Van de Peer Y, Wincker P (2010) The *Ectocarpus* genome and the independent evolution of multicellularity in brown algae. Nature 465(7298):617–621. doi:10.1038/nature09016

Coelho SM, Scornet D, Rousvoal S, Peters NT, Dartevelle L, Peters AF, Cock JM (2012) *Ectocarpus*: a model organism for the brown algae. Cold Spring Harb Protoc 2012(2):193–198. doi:10.1101/pdb.emo065821

Coimbra S, Almeida J, Junqueira V, Costa ML, Pereira LG (2007) Arabinogalactan proteins as molecular markers in *Arabidopsis thaliana* sexual reproduction. J Exp Bot 58(15–16):4027–4035. doi:10.1093/jxb/erm259

Deniaud-Bouët E, Kervarec N, Michel G, Tonon T, Kloareg B, Hervé C (2014) Chemical and enzymatic fractionation of cell walls from Fucales: insights into the structure of the extracellular matrix of brown algae. Ann Bot 114(6):1203–1216. doi:10.1093/aob/mcu096

Domozych DS (2012) The quest for a four-dimensional imaging in plant cell biology: it's just a matter of time. Ann Bot 110(2):461–474. doi:10.1093/aob/mcs107

Domozych DS, Lambiasse L (2009) Cell-wall development and bipolar growth in the desmid *Penium margaritaceum* (Zygnematophyceae, Streptophyta). Asymmetry in a symmetric world. J Phycol 45(4):879–893. doi:10.1111/j.1529-8817.2009.00713.x

Domozych DS, Serfis A, Kiemle SN, Gretz MR (2007) The structure and biochemistry of charophycean cell walls: I. Pectins of *Penium margaritaceum*. Protoplasma 230(1–2):99–115. doi:10.1007/s00709-006-0197-8

Domozych DS, Brechka H, Britton A, Toso M (2011) Cell wall growth and modulation dynamics in a model unicellular green alga—*Penium margaritaceum*: live cell labeling with monoclonal antibodies. J Bot 2011:1–8. doi:10.1155/2011/632165, Article ID 632165

Dubois M, Gilles KA, Hamilton JK, Rebers PA, Smith F (1956) Colorimetric method for determination of sugars and related substances. Anal Chem 28(3):350–356

Enquist-Newman M, Faust AM, Bravo DD, Santos CN, Raisner RM, Hanel A, Sarvabhowman P, Le C, Regitsky DD, Cooper SR, Peereboom L, Clark A, Martinez Y, Goldsmith J, Cho MY, Donohoue PD, Luo L, Lamberson B, Tamrakar P, Kim EJ, Villari JL, Gill A, Tripathi SA, Karamchedu P, Paredes CJ, Rajgarhia V, Kotlar HK, Bailey RB, Miller DJ, Ohler NL, Swimmer C, Yoshikuni Y (2014) Efficient ethanol production from brown macroalgae sugars by a specific yeast platform. Nature 505(7482):239–243. doi:10.1038/nature12771

Estevez JM, Leonardi PI, Alberghina JS (2008) Cell wall carbohydrate epitopes in the green alga *Oedogonium bharuchae* F. *minor* (Oedogoniales, Chlorophyta). J Phycol 44(5):1257–1268. doi:10.1111/j.1529-8817.2008.00568.x

Estevez JM, Fernández PV, Kasulin L, Dupree P, Ciancia M (2009) Chemical and *in situ* characterization of macromolecular components of the cell walls from the green seaweed *Codium fragile*. Glycobiology 19(3):212–228. doi:10.1093/glycob/cwn101

Evans NA, Hoyne PA, Stone BA (1984) Characteristics and specificity of the interaction of a fluorochrome from aniline blue (sirofluor) with polysaccharides. Carbohydr Res 4(3):215–230. doi:10.1016/0144-8617(84)90012-2

Falter C, Zwikowics C, Eggert D, Blümke A, Naumann M, Wolff K, Ellinger D, Reimer R, Voigt CA (2015) Glucanocellulosic ethanol: the undiscovered biofuel potential in energy crops and marine biomass. Scie Rep 5:13722. doi:10.1038/srep13722

Ferguson C, Teeri TT, Siika-aho M, Read SM, Bacic A (1998) Location of cellulose and callose in pollen tubes and grains of *Nicotiana tabacum*. Planta 206(3):452–460. doi:10.1007/s004250050421

Fernández PV, Ciancia M, Miravalles AB, Estevez JM (2010) Cell-wall polymer mapping in the coenocytic macroalga *Codium vermilara* (Bryopsidales, Chlorophyta). J Phycol 46(3):456–465. doi:10.1111/j.1529-8817.2010.00821.x

Geitmann A, Hudák J, Vennigerholz F, Walles B (1995) Immunogold localization of pectin and callose in pollen grains and pollen tubes of *Brugmansia suaveolens*—implications for the self-incompatibility reaction. J Plant Physiol 147(2):225–235. doi:10.1016/S0176-1617(11)81509-9

Graham LE, Wilcox LW (2000) Algae. Prentice Hall, New York

Green JR, Stafford CJ, Jones JL, Wright PJ, Callow JA (1993) Binding of monoclonal antibodies to vegetative tissue and fucose-containing polysaccharides of *Fucus serratus* L. New Phytol 124(3):397–408. doi:10.1111/j.1469-8137.1993.tb03830.x

Guibet M, Boulenguer P, Mazoyer J, Kervarec N, Antonopoulos A, Lafosse M, Helbert W (2008) Composition and distribution of carrabiose moieties in hybrid k-/i-carrageenans using carrageenases. Biomacromolecules 9(1):408–415. doi:10.1021/bm701109r

Haug A (1964) Composition and properties of alginates. Norwegian Institute of Technology, Trondheim

Herburger K, Holzinger A (2015) Localization and quantification of callose in the streptophyte green algae *Zygnema* and *Klebsormidium*: correlation with desiccation tolerance. Plant Cell Physiol 56(11):2259–2270. doi:10.1093/pcp/pcv139

Hibberd DJ, Norris RE (1984) Cytology and ultrastructure of *Chlorarachnion reptans* (Chlorarachniophyta Divisio Nova, Chlorarachniophyceae Classis Nova). J Phycol 20(2):310–330. doi:10.1111/j.0022-3646.1984.00310.x

Humbel BM, Konomi M, Takagi T, Kamasawa N, Ishijima SA, Osumi M (2001) *In situ* localization of β-glucans in the cell wall of *Schizosaccharomyces pombe*. Yeast 18:433–444

Jones JL, Callow JA, Green JR (1988) Monoclonal antibodies to sperm surface antigens of the brown alga *Fucus serratus* exhibit region-, gamete-, species- and genus-preferential binding. Planta 176(3):298–306. doi:10.1007/BF00395410

Kadam SU, O'Donnel CP, Rai DK, Hossain MB, Burgess CM, Walsh D, Tiwari BK (2015) Laminarin from Irish brown seaweeds *Ascophyllum nodosum* and *Laminaria hyperborea*: ultrasound assisted extraction, characterization and bioactivity. Mar Drugs 13:4270–4280. doi:10.3390/md13074270

Kauss H (1989) Fluorometric measurement of callose and other 1,3-β-glucans. p127–136. In: Linskens HF, Jackson JF (eds) Plant fibers. Modern methods of plant analysis. New series, vol 10. Springer Press, Berlin

Kauss H (1996) Callose synthesis. In: Smallwood M, Knox JP, Bowles DJ (eds) Membranes: specialized functions in plants. BIOS Scientific Publishers, Guildford, pp 77–92

Kim D-S, Park Y-H (1985) Uronic acid composition, block structure and some related properties of alginic acid (3) on alginic acid prepared from *Sargassum ringgoldianum*. J Korean Fish Soc 18(1):29–36

Kloareg B, Quatrano RS (1988) Structure of cell walls of marine algae and ecophysiological functions of the matrix polysaccharides. Oceanogr Mar Biol Annu Rev 26:259–315

Knoblauch J, Drobnitch TS, Peters WS, Knoblauch M (2016) *In situ*-microscopy reveals reversible cell wall swelling in kelp sieve tubes: one mechanism for turgor generation and flow control? Plant Cell Environ 39(8):1727–1736. doi:10.1111/pce.12736

Knox JP (1997) The use of antibodies to study the architecture and developmental regulation of plant cell walls. Int Rev Cytol 171:79–120. doi:10.1016/S0074-7696(08)62586-3

Knox JP, Benitez-Alfonso Y (2014) Roles and regulation of plant cell walls surrounding plasmodesmata. Curr Opin Plant Biol 22:93–100. doi:10.1016/j.pbi.2014.09.009

Kropf DL, Kloareg B, Quatrano RS (1988) Cell wall is required for fixation of the embryonic axis in *Fucus* zygotes. Science 239(4836):187–190. doi:10.1126/science.3336780

Lahaye M, Jegou D, Buleon A (1994) Chemical characteristics of insoluble glucans from the cell wall of the marine green alga *Ulva lactuca* (L.) Thuret. Carbohydr Res 262(1):115–125. doi:10.1016/0008-6215(94)84008-3

Lechat H, Amat M, Mazoyer J, Buléon A, Lahaye M (2000) Structure and distribution of glucomannan and sulfated glucan in the cell walls of the red alga *Kappaphycus alvarezii* (Gigartinales, Rhodophyta). J Phycol 36(5):891–902. doi:10.1046/j.1529-8817.2000.00056.x

Lee RE (2008) Phycology, 4th edn. Cambridge University Press, Cambridge

Lee KJD, Marcus SE, Knox JP (2011) Cell wall biology: perspectives from cell wall imaging. Mol Plant 4(2):212–219. doi:10.1093/mp/ssq075

Li B, Lu F, Wei X, Zhao R (2008) Fucoidan: structure and bioactivity. Molecules 13(8):1671–1695. doi:10.3390/molecules13081671

Lobban CS, Harrison PJ (1994) Seaweed ecology and physiology. Cambridge University Press, Cambridge

Ludwig M, Gibbs SP (1989) Evidence that the nucleomorphs of *Chlorarachnion reptans* (Chlorarachniophyceae) are vestigial nuclei: morphology, division and DNA-DAPI fluorescence. J Phycol 25(2):385–394. doi:10.1111/j.1529-8817.1989.tb00135.x

Mabeau S, Kloareg B (1987) Isolation and analysis of the cell walls of brown algae: *Fucus spiralis*, *F. ceranoides*, *F. vesiculosus*, *F. serratus*, *Bifurcaria bifurcata* and *Laminaria digitata*. J Exp Bot 38(9):1573–1580. doi:10.1093/jxb/38.9.1573

Masuko T, Minami A, Iwasaki N, Majima T, Nishimura S-I, Lee YC (2005) Carbohydrate analysis by a phenol-sulfuric acid method in microplate format. Anal Biochem 339(1):69–72. doi:10.1016/j.ab.2004.12.001

McCully ME (1965) A note on the structure of the cell walls of the brown alga Fucus. Can J Bot 43(8):1001–1004. doi:10.1139/b65-114

McCully ME, Goff LJ, Adshead PC (1980) Preparation of algae for light microscopy. In: Gantt E (ed) Handbook of phycological methods: developmental and cytological methods. Cambridge University Press, Cambridge, pp 263–281

McFadden GI, Gilson PR, Hofmann CJB, Adcock GJ, Maier UG (1994) Evidence that an amoeba acquired a chloroplast by retaining part of an engulfed eukaryotic alga. Proc Natl Acad Sci U S A 91(9):3690–3694

McFadden GI, Gilson PR, Sims IM (1997) Preliminary characterization of carbohydrate stores from chlorarachniophytes (Division: Chlorarachniophyta). Phycol Res 45(3):145–151. doi:10.1111/j.1440-1835.1997.tb00087.x

Meikle PJ, Bonig I, Hoogenraad NJ, Clarke AE, Stone BA (1991) The location of (1→3)-β-glucans in the walls of pollen tubes of *Nicotiana alata* using a (1→3)-β-glucan-specific monoclonal antibody. Planta 185(1):1–8. doi:10.1007/BF00194507

Meikle PJ, Hoogenraad NJ, Bonig I, Clarke AE, Stone BA (1994) A (1→3, 1→4)-β-glucan-specific monoclonal antibody and its use in the quantification and immunocytochemical location of (1→3, 1→4)-β-glucans. Plant J 5(1):1–9. doi:10.1046/j.1365-313X.1994.5010001.x

Mian AJ, Percival E (1973) Carbohydrates of the brown seaweeds *Himanthalia lorea*, *Bifurcaria bifurcata*, and *Padina pavonia*. Carbohydr Res 26(1):133–146

Michel G, Tonon T, Scornet D, Cock JM, Kloareg B (2010a) The cell wall polysaccharide metabolism of the brown alga *Ectocarpus siliculosus*. Insights into the evolution of extracellular matrix polysaccharides in Eukaryotes. New Phytol 188(1): 82–97. doi:10.1111/j.1469-8137.2010.03374.x

Michel G, Tonon T, Scornet D, Cock JM, Kloareg B (2010b) Central and storage carbon metabolism of the brown alga *Ectocarpus siliculosus*: insights into the origin and evolution of storage carbohydrates in Eukaryotes. New Phytol 188(1):67–81. doi:10.1111/j.1469-8137.2010.03345.x

Moller I, Sørensen I, Bernal AJ, Blaukopf C, Lee K, Øbro J, Pettolino F, Roberts A, Mikkelsen JD, Knox JP, Bacic A, Willats WGT (2007) High-throughput mapping of cell-wall polymers within and between plants using novel microarrays. Plant J 50(6):1118–1128. doi:10.1111/j.1365-313X.2007.03114.x

Moller I, Marcus SE, Haeger A, Verhertbruggen Y, Verhoef R, Schols H, Ulvskov P, Mikkelsen JD, Knox JP, Willats W (2008) High-throughput screening of monoclonal antibodies against plant cell wall glycans by hierarchical clustering of their carbohydrate microarray binding profiles. Glycoconj J 25(1):37–48. doi:10.1007/s10719-007-9059-7

Moller IE, Pettolino FA, Hart C, Lampugnani ER, Willats WGT, Bacic A (2012) Glycan profiling of plant cell wall polymers using microarrays. J Vis Exp 70(e4238):1–9. doi:10.3791/4238

Mollet J-C, Leroux C, Dardelle F, Lehner A (2013) Cell wall composition, biosynthesis and remodeling during pollen tube growth. Plants 2(1):107–147. doi:10.3390/plants2010107

Moss BL (1983) Sieve elements in the Fucales. New Phytol 93(3):433–437

Naylor GL, Russel-Wells B (1934) On the presence of cellulose and its distribution in the cell-walls of brown and red algae. Ann Bot 48(3): 635–641

Niklas KJ (2004) The cell walls that bind the tree of life. Bioscience 54(9): 831–841. doi:10.1641/0006-3568(2004)054[0831:TCWTBT]2.0.CO;2

Nitschke U, Stengel DB (2015) A new HPLC method for the detection of iodine applied to natural samples of edible seaweeds and commercial seaweed food products. Food Chem 172: 326–334. doi:10.1016/j.foodchem.2014.09.030

Nitschke U, Dixneuf S, Ruth AA, Schmid M, Stengel DB (2013) Molecular iodine ($I_2$) emission from two Laminaria species (Phaeophyceae) and impact of irradiance and temperature on $I_2$ emission into air and iodide release into seawater from *Laminaria digitata*. Mar Environ Res 92:102–109. doi:10.1016/j.marenvres.2013.09.006

Norton TA, Melkonian M, Andersen RA (1996) Algal biodiversity. Phycologica 35(4):308–326. doi:10.2216/i0031-8884-35-4-308.1

Novotny AM, Forman M (1975) The composition and development of cell walls of *Fucus* embryos. Planta 122:67–78

Park EP, Díaz-Moreno SM, Davis DJ, Wilkop TE, Bulone V, Drakakaki G (2015) Endosidin 7 specifically arrests late cytokinesis and inhibits callose biosynthesis, revealing distinct trafficking events during cell plate maturation. Plant Physiol 165(3):1019–1034. doi:10.1104/pp.114.241497

Patankar MS, Oehninger S, Barnett T, Williams RL, Clark GF (1993) A revised structure for fucoidan may explain some of its biological activities. J Biol Chem 268(29):21770–21776

Pattathil S, Avci U, Baldwin D, Swennes AG, McGill JA, Popper Z, Booten T, Albert A, Davis RH, Chennareddy C, Dong R, O'Shea B, Rossi R, Leoff C, Freshour G, Narra R, O'Neill M, York WS, Hahn MG (2010) A comprehensive toolkit of plant cell wall glycan-directed monoclonal antibodies. Plant Physiol 153(2):514–525. doi:10.1104/pp.109.151985

Pattathil S, Avci U, Miller JS, Hahn MG (2012) Immunological approaches to plant cell wall and biomass characterization: glycome profiling. In: Himmel ME (ed) Biomass conversion: methods and protocols, vol 908. Methods in molecular biology. Humana, pp 61–72. doi:10.1007/978-1-61779-956-3_6

Pattathil S, Avci U, Zhang T, Cardenas CL, Hahn MG (2015) Immunological approaches to biomass characterization and utilization. Front Bioeng Biotechnol 3:173. doi:10.3389/fbioe.2015.00173

Patterson DJ (1999) The diversity of Eukaryotes. Am Nat 154(S4):S96–S124. doi:10.1086/303287

Pennington W (1937) The secondary thickening of *Fucus*. New Phytol 36:267–279

Percival E (1979) The polysaccharides of green, red and brown seaweeds—their basic structure, biosynthesis and function. Br Phycol J 14(2):103–117. doi:10.1080/00071617900650121

Popper ZA, Michel G, Hervé C, Domozych DS, Willats WGT, Tuohy MG, Kloareg B, Stengel DB (2011) Evolution and diversity of plant cell walls: from algae to flowering plants. Annu Rev Plant Biol 62: 567–590. doi:10.1146/annurev-arplant-042110-103809

Quatrano RS, Stevens PT (1976) Cell wall assembly in *Fucus* zygotes. I. Characterization of the polysaccharide components. Plant Physiol 58(2):224–231. doi:10.1104/pp.58.2.224

Rabanal M, Ponce NMA, Navarro DA, Gómez RM, Stortz CA (2014) The system of fucoidans from the brown seaweed *Dictyota dichotoma*: chemical analysis and antiviral activity. Carbohydr Polym 101:804–811. doi:10.1016/j.carbpol.2013.10.019

Radford JE, Vesk M, Overall RL (1998) Callose deposition in plasmodesmata. Protoplasma 201(1–2):30–37. doi:10.1007/BF01280708

Raimundo SC, Avci U, Hopper C, Pattathil S, Hahn MG, Popper ZA (2016) Immunolocalization of cell wall carbohydrate epitopes in seaweeds: presence of land plant epitopes in *Fucus vesiculosus* L. (Phaeophyceae). Planta 243(2):337–354. doi:10.1007/s00425-015-2412-3

Read SM, Currie G, Bacic A (1996) Analysis of the structural heterogeneity of laminarin by electrospray-ionisation-mass spectrometry. Carbohydr Res 281(2):187–201. doi:10.1016/0008-6215(95)00350-9

Rioux L-E, Turgeon SL, Beaulieu M (2007) Characterization of polysaccharides extracted from brown seaweeds. Carbohydr Polym 69(3): 530–537. doi:10.1016/j.carbpol.2007.01.009

Ropartz D, Giuliani A, Hervé C, Geairon A, Jam M, Czjzek M, Rogniaux H (2015) High-energy photon activation tandem mass spectrometry provides unprecedented insights into the structure of highly sulfated oligosaccharides extracted from macroalgal cell walls. Anal Chem 87(2):1042–1049. doi:10.1021/ac5036007

Schaal G, Leclerc J-C, Droual G, Leroux C, Riera P (2016) Biodiversity and trophic structure of invertebrate assemblages associated with understorey red algae in a *Laminaria digitata* bed. Mar Biol Res 12(5):513–523. doi:10.1080/17451000.2016.1164318

Schiel DR, Foster MS (2006) The population biology of large brown seaweeds: ecological consequences of multiphase life histories in dynamic coastal environments. Annu Rev Ecol Evol Syst 37:343–372. doi:10.1146/annurev.ecolsys.37.091305.110251

Schmitz K, Lobban CS (1976) A survey of translocation in Laminariales (Phaeophyceae). Mar Biol 36(3):207–216

Schmitz K, Srivastava LM (1976) The fine structure of sieve elements of *Nereocystis lütkeana*. Am J Bot 63(5):679–693

Schoenwaelder MEA (2008) The biology of phenolic containing vesicles. Algae 23(3):163–175

Schultze K, Janke K, Krüß A, Weidemann W (1990) The macrofauna and macroflora associated with *Laminaria digitata* and *L. hyperborea* at the island of Helgoland (German Bight, North Sea). Helgoländer Meeresunters 44:39–51

Smidsrød O, Glover RM, Whittington SG (1973) The relative extension of alginates having different chemical composition. Carbohydr Res 27:107–118

Smith AI (1939) The comparative histology of some of the Laminariales. Am J Bot 26(8):571–585

Smith MM, McCully ME (1978) A critical evaluation of the specificity of aniline blue induced fluorescence. Protoplasma 95:229–254

Stengel DB, Connan S, Popper ZA (2011) Algal chemodiversity and bioactivity: sources of natural variability and implications for commercial application. Biotechnol Adv 29(5):483–501. doi:10.1016/j.biotechadv.2011.05.016

Stiller JW, Huang J, Ding Q, Tian J, Goodwillie C (2009) Are algal genes in nonphotosynthetic protists evidence of historical plastid endosymbioses? BMC Genomics 10(484):1–16. doi:10.1186/1471-2164-10-484

Stone BA (2009) Chemistry of β-glucans. In: Bacic A, Fincher GB, Stone BA (eds) Chemistry, biochemistry, and biology of (1–3)-β-glucans and related polysaccharides. Academic, San Diego, pp 5–46. doi:10.1016/B978-0-12-373971-1.00002-9

Stone BA, Clarke AE (1992) Chemistry and physiology of higher plant (1, 3)-β-glucans (callose). In: Stone BA, Clark A (eds) Chemistry and biology of (1,3)-β-glucans. La Trobe University Press, Bundoora, pp 365–429

Stone BA, Evans NA, Bonig I, Clarke AE (1984) The application of Sirofluor, a chemically defined fluorochrome from aniline blue for the histochemical detection of callose. Protoplasma 122(3):191–195. doi:10.1007/BF01281696

Suzuki E, Suzuki R (2013) Variations of storage polysaccharides in phototrophic microorganisms. J Appl Glycosci 60:21–27. doi:10.5458/jag.jag.JAG-2012_016

Sykes MG (1908) Anatomy and histology of *Macrocystis pyrifera* and *Laminaria saccharina*. Ann Bot 22(2):291–325

Tanaka A, Nagasato C, Uwai S, Motomura T, Kawai H (2007) Re-examination of ultrastructure of the stellate chloroplast organization in brown algae: structure and development of pyrenoids. Phycol Res 55(3):203–213. doi:10.1111/j.1440-1835.2007.00463.x

Team RDC (2011) A language and environment for statistical computing. R Foundation for Statistical Computing, Vienna

Tesson B, Charrier B (2014) Brown algal morphogenesis: atomic force microscopy as a tool to study the role of mechanical forces. Front Plant Sci 5(471):1–7. doi:10.3389/fpls.2014.00471

Torode TA, Marcus SE, Jam M, Tonon T, Blackburn RS, Hervé C, Knox JP (2015) Monoclonal antibodies directed to fucoidan preparations from brown algae. PLoS One 10(2):e0118366. doi:10.1371/journal.pone.0118366

Tsirigoti A, Beakes GW, Hervé C, Gachon CMM, Katsaros C (2015) Attachment, penetration and early host defense mechanisms during the infection of filamentous brown algae by *Eurychasma dicksonii*. Protoplasma 252(3):845–856. doi:10.1007/s00709-014-0721-1

Usov AI, Bilan MI (2009) Fucoidans—sulfated polysaccharides of brown algae. Russ Chem Rev 78(8):785–799

Van Went JL, Tammes PML (1973) Trumpet filaments in *Laminaria digitata* as an artefact. Acta Bot Neerlandica 22(2):112–119

Van Went JL, Van Aelst AC, Tammes PML (1973) Open plasmodesmata in sieve plates of *Laminaria digitata*. Acta Bot Neerlandica 22(2):120–123

Vreeland V (1970) Localization of a cell wall polysaccharide in a brown alga with labeled antibody. J Histochem Cytochem 18(5):371–373. doi:10.1177/18.5.371

Vreeland V (1972) Immunocytochemical localization of the extracellular polysaccharide alginic acid in the brown seaweed, *Fucus distichus*. J Histochem Cytochem 20(5):358–367. doi:10.1177/20.5.358

Vreeland V, Slomich M, Laetsch WM (1984) Monoclonal antibodies as molecular probes for cell wall antigens of the brown alga, *Fucus*. Planta 162(6):506–517. doi:10.1007/BF00399916

Vreeland V, Zablackis E, Laetsch WM (1992) Monoclonal antibodies as molecular markers for the intracellular and cell wall distribution of carrageenan epitopes in *Kappaphycus* (Rhodophyta) during tissue development. J Phycol 28(3):328–342. doi:10.1111/j.0022-3646.1992.00328.x

Wargacki AJ, Leonard E, Win MN, Regitsky DD, Santos CNS, Kim PB, Cooper SR, Raisner RM, Herman A, Sivitz AB, Lakshmanaswamy A, Kashiyama Y, Baker D, Yoshikuni Y (2012) An engineered microbial platform for direct biofuel production from brown macroalgae. Science 335(6066):308–313. doi:10.1126/science.1214547

Willats WGT, Steele-King CG, McCartney L, Orfila C, Marcus SE, Knox JP (2000) Making and using antibody probes to study plant cell walls. Plant Physiol Biochem 38(1–2):27–36. doi:10.1016/S0981-9428(00)00170-4

Wood PJ, Fulcher RG (1984) Specific interaction of aniline blue with (1→3)-β-D-glucan. Carbohydr Polym 4(1):49–72. doi:10.1016/0144-8617(84)90044-4

Xie B, Wang X, Zhu M, Zhang Z, Hong Z (2011) CalS7 encodes a callose synthase responsible for callose deposition in the phloem. Plant J 65(1):1–14. doi:10.1111/j.1365-313X.2010.04399.x

Yamaguchi T, Ikawa T, Nisizawa K (1966) Incorporation of radioactive carbon from $H^{14}CO_3^-$ into sugar constituents by a brown alga, *Eisenia bicyclis*, during photosynthesis and its fate in the dark. Plant Cell Physiol 7(2):217–229

Yamanouchi S (1908) Sieve tubes in Laminariales. Bot Gaz 46(2):153–154

Yoon HS, Hackett JD, Ciniglia C, Pinto G, Bhattacharya D (2004) A molecular timeline for the origin of photosynthetic Eukaryotes. Mol Biol Evol 21(5):809–818. doi:10.1093/molbev/msh075

Zavaliev R, Ueki S, Epel B, Citovsky V (2011) Biology of callose (β-1,3-glucan) turnover at plasmodesmata. Protoplasma 248(1):117–130. doi:10.1007/s00709-010-0247-0

Zhao D, Zhuo RX, Cheng SX (2012) Alginate modified nanostructured calcium carbonate with enhanced delivery efficiency for gene and drug delivery. Mol BioSyst 8(3):753–759. doi:10.1039/c1mb05337j